

Reliability Analysis of Grate Inlets

by

`Aifaa Balqis binti Kamarul Zaman

19241

Dissertations submitted in partial fulfilment of

the requirements for the

Bachelor of Engineering (Hons)

(Civil Engineering)

SEPTEMBER 2017

Universiti Teknologi PETRONAS

32610 Seri Iskandar,

Perak Darul Ridzuan,

Malaysia

CERTIFICATION OF APPROVAL

Reliability Analysis of Grate Inlets

by

`Aifaa Balqis binti Kamarul Zaman

19241

A project dissertation submitted to the

Civil Engineering Programme

Universiti Teknologi PETRONAS

in partial fulfilment of the requirements for the

BACHELOR OF ENGINEERING (Hons)

CIVIL

Approved by,

(Assoc. Prof. Dr. Zahiraniza Mustaffa)

UNIVERSITI TEKNOLOGI PERTRONAS

TRONOH, PERAK

September 2017

CERTIFICATION OF ORIGINALITY

This is to certify that I am responsible for the work submitted in this project, that the original work is my own except as specified in the references and acknowledgement and that the original work contained herein have not been undertaken or done by unspecified sources or persons.

`AIFAA BALQIS KAMARUL ZAMAN

ABSTRACT

Street inlet is a drainage structure with an opening used to collect stormwater runoff from the street pavement and discharge it into a stormwater drainage system. In Malaysia, urbanization has led to the use of concrete structures and pavement which reduce the infiltration rate of stormwater into the ground. During a high stormwater event, the street inlet fails to intercept the water and lead to street ponding. This research is conducted to investigate the hydraulic efficiency of three grate inlet designs used in Malaysia and develop a reliability model to determine the probability of failure of the grate inlets. In this experimental study, a full scale of half way roadway flume was used to simulate flows of the stormwater into the grate inlets. The efficiency of each grate inlets was analysed at different approaching flows. Results showed that the ability of each inlet to capture and intercept the flow is varies, thus resulting in different hydraulic efficiency. It is also found that the longitudinal grate inlet performs better than transverse inlet and the larger the length dimension of the grate, the higher the efficiency. As the approaching flow increases, the hydraulic efficiency of the inlet decreases. The results from the experiments were then used to develop a new reliability model and able to be used as a guide for inlet designs for Department of Irrigation and Drainage (DID) in Malaysia which also aims at improving the current MSMA guideline.

ACKNOWLEDGEMENT

Upon the completion of this research, I would like to express my gratitude to my FYP Supervisor, Assoc. Prof. Dr. Zahiraniza Mustaffa for your guidance and patience throughout my research. Thank you for sharing your knowledge and words of motivation which have been an encouragement and self-motivation to myself to finish the research. This research would not have been possible without your constant support.

Much appreciation also goes to Mr. Idris Mokhtar, Mr. Mohd Zaid bin Zainuddin and Mr. Meor Asniwan bin Mew Ghazali, Lab Technologists of Civil Engineering Lab Facilities Services Unit. Thank you so much for your cooperation in giving technical assistance and guidance throughout my experiment in the Hydraulics Lab.

Next, I would like to give a special appreciation to Ms. Amirah Husna bt Abdul Halim, a Master student of Dr Zahiraniza for your kind assistance in sharing knowledge and guidance to use MATLAB software.

Special thanks also go to my fellow colleagues, Nur Muhammad Hadri Che Hassan, Mc Dalglish Virody Lajitan and Nor Haslinayati Abdul Ghafar for your kindness and patience. Thank you for your willingness to spend time and help my research.

I would like to express my gratitude to my family and friends for their continuous support in giving motivation, loves and prayers throughout my journey to graduation. Last but not least, an acknowledgement to Universiti Teknologi PETRONAS for providing a great platform for their students to conduct research and thus enhance students' skills in applying knowledge, solving problems and presenting findings of their research.

TABLE OF CONTENTS

CERTIFICATION OF APPROVAL	I
CERTIFICATION OF ORIGINALITY	II
ABSTRACT	III
ACKNOWLEDGEMENT	IV
TABLE OF CONTENTS	V
LIST OF FIGURES	VII
LIST OF TABLES	IX
CHAPTER 1 INTRODUCTION	1
1.1 Background of Study	1
1.2 Problem Statement	2
1.3 Objectives	3
1.4 Scope of Study	3
CHAPTER 2 LITERATURE REVIEW	4
2.1 Introduction	4
2.2 Street Inlet	4
2.2.1 Grate Inlet	5
2.2.2 Curb Opening Inlet	6
2.2.3 Combination Inlet	7
2.3 Advantages and Disadvantages of Street Inlets	8
2.4 Street Pavement Drainage	9
2.5 Location of Street Inlets	10
2.5.1 Grate Inlet on Grade	11
2.5.2 Grate Inlet in Sump	11
2.6 Governing Equations of Street Inlets	12
2.6.1 Weir Flow	12
2.6.2 Orifice flow	14
2.6.3 Froude Number	14
2.7 Studies of Street Inlets	15
2.8 Random Variable and Probability Distribution	17
2.9 Standard Normal Distribution	17
2.10 Limit State Function, Strength and Load	18

2.11 Monte Carlo Simulation	19
CHAPTER 3 RESEARCH METHODOLOGY	21
3.1 Introduction	21
3.2 Research Flow	21
3.3 Selection of Grate Inlet Designs.....	22
3.4 Experimental Set Up	23
3.4.1 Half Roadway Flume	23
3.4.2 Types of Tank	24
3.4.3 Flows of Experiments	26
3.5 Development of Limit State Function	28
3.6 Simulation of Limit State Function (LSF) Model	29
CHAPTER 4 RESULTS AND DISUSSION.....	31
4.1 Introduction	31
4.2 Efficiency of Grate Inlets	31
4.3 Probability of Failure of Grate Inlets	34
4.4 Observation	39
CHAPTER 5 CONCLUSIONS AND RECOMMENDATIONS	44
REFERENCES.....	45
APPENDIX	48

LIST OF FIGURES

Figure 1.1: Ponding street	1
Figure 2.1: Grate inlet (Adapted & revised from Guo, 1997).....	5
Figure 2.2: Grate inlet design with (a) longitudinal and (b) transverse grate	6
Figure 2.3: Curb opening inlet (Adapted & revised from Guo, 1997).....	7
Figure 2.4: Curb-opening inlet (a) undepressed and (b) depressed	8
Figure 2.5: Combination inlet (Adapted & revised from Guo, 1997	8
Figure 2.6: Clogged grate inlet.....	8
Figure 2.7: Composite gutter cross section.....	9
Figure 2.8: Location of Street Inlet (Adapted from Guo, 1997)	10
Figure 2.9: Sharp-crested weir.....	13
Figure 2.10: Types of weir (a) rectangular weir and (b) triangular weir	13
Figure 2.11: Standard Normal Distribution Function.....	18
Figure 3.1: Three different design of (a) grate inlet 1, (b) grate inlet 2 and (c) grate inlet 3	22
Figure 3.2: Bar configurations of (a) grate inlet 1, (b) grate inlet 2 and (c) grate inlet 3	22
Figure 3.3: Half Roadway Flume Setup.....	23
Figure 3.4: Types of weir	24
Figure 3.5: (a) Actual and (b) 3D drawing of rectangular weir	25
Figure 3.6: (a) Actual and (b) 3D drawing of V-notch Weir.....	25
Figure 3.7: Sketch of the plan view of the half roadway flume	26
Figure 3.8: Summary of the experiment.....	27
Figure 3.9: Code in the script editor	29
Figure 3.10: Run the program.....	30
Figure 3.11: Probability of failure of grate inlet simulation.....	33
Figure 4.1: Graph of efficiency, η vs approaching flow, Q_a	35
Figure 4.2: Graph of probability of failure against approaching flow	36
Figure 4.3: Graph of probability of failure against efficiency.....	37
Figure 4.4: Graph of probability of failure against Froude number	39
Figure 4.6: (a) grate inlet 1, (b) grate inlet 2 and (c) grate inlet 3 capturing approaching flow	40

Figure 4.7: Bypass flow at (a) minimum flow and (b) maximum flow	40
Figure 4.8: Actual flow state at (a) minimum flow and (b) maximum flow	41
Figure 4.9: Illustration of flow interception at (a) minimum and (b) maximum flows.....	41
Figure 4.10: Actual water spreads at (a) minimum and (b) maximum flows.....	42
Figure 4.11: Illustration of water spreads at minimum flow	42
Figure 4.12: Illustration of water spread at maximum flow	43

LIST OF TABLES

Table 3.1: Grate inlets specifications	22
Table 3.2: Descriptive statistics of failure of grate inlets.....	28
Table A.1: Efficiency of grate inlets	48
Table A.2: Approaching flow and Probability of failure of grate inlets	48
Table A.3: Efficiency and Probability of failure of grate inlets.....	49
Table A.4: Froude number and Probability of failure of grate inlets.....	49

CHAPTER 1

INTRODUCTION

1.1 Background of Study

Street pavements are made to facilitate the traffic movement. Besides, it is also to be part of the storm water drainage system which provides drainage function during a storm event. In an urban street, the excessive storm water runoff will flow from the street crown to the street curb. Then, street gutter will collect and intercept the storm water into an opening structure known as street inlet. The street inlet is an important drainage structure that collects and removes storm water from street pavement. It is essential to properly design, install and maintain the street inlet to avoid from stormwater ponding and flood on the street pavement. As shown in the Figure 1.1, street ponding or flood occurrence on the pavement can cause traffic hazard whereby it will slow traffic, hydroplaning and loss of visibility (Guo, 1997) which lead to accidents for the street user.



Figure 1.1: Ponding street

There are several types of street inlet and each of it has different design in term of pattern, sizes and configurations. In Malaysia, there are two typical types of street inlet installed along the street pavement namely grate inlet and curb-opening inlet. Each of the inlets has its own design to suit the street conditions. There are many factors that can affect the street inlet performance. From design aspects, factors that can affect the performance might be from the hydraulics of the surface flow, hydraulic behaviour of drainage structures (rainfall patterns and hydrological conditions), inlet hydraulic capacity and in case of storm, hazard criteria related to urban runoff also need to be considered (Russo and et al., 2013).

This research was carried out to study the hydraulic efficiency of several typical grate inlets used in Malaysia. Experimental studies were conducted in the laboratory of Universiti Teknologi PETRONAS to obtain data to measure the hydraulic efficiency of the street inlet. Based on the efficiencies, the performance of inlets by referring to the total street flow percentage that able to be intercepted by the inlet were reported accordingly.

In addition, this research was also conducted to study the reliability analysis of different grate inlet designs considering the uncertainties in measuring the flows captured by the inlet. In drainage design, uncertainty often leads to under or overuse of inlet design (Comport & Thornton, 2012). Therefore, in order to understand the performance of each grate inlet design, experimental data collected from laboratory works would will be incorporated in a consistent manner for reliability analysis. This research would eventually report on the probability of failures of each inlet tested

1.2 Problem Statement

The urban streets pavement in Malaysia was equipped with various types of street inlet design. The problem of these street inlets is that during a high stormwater event, street pavement ponding occurs when the street inlet fails to intercept the stormwater due to clogging or improper design and installation. Water is accumulating around the street inlets and it can interrupt traffic and sometimes contributes to accident from loss of visibility and hydroplaning.

In Malaysia, the hydraulic efficiency of street inlet to intercept the stormwater are not yet studied thoroughly. Thus, this research is important to describe the hydraulic performance of the incoming flows into the grate inlet before it starts to accumulate around the inlet and spread to the street pavement. Based on the hydraulic performance, a reliability model will be developed to understand the probability of failure each of the selected grate inlets.

1.3 Objectives

1. To experimentally study the hydraulic efficiency of several typical grate inlets in Malaysia.
2. To propose a reliability model of the grate inlet design based on data obtained from the experimental studies.

1.4 Scope of Study

The scope of study for this research is conducting experimental studies on three grate inlet designs. It comprises the study of type of grate inlet used in Malaysia, typical road design in Malaysia and governing equation of grate inlet.

Besides, this research also studies the reliability of street inlet design. It applies knowledge of the probabilistic approach to compute the probability of failure for each street inlet design. This approach involved limit state function, probability of density function and MATLAB for simulation.

CHAPTER 2

LITERATURE REVIEW

2.1 Introduction

This chapter presents a literature review on different types of street inlet used in an urban street pavement and advantages and disadvantages of street inlets. Throughout the chapter, the focus will be more on grate inlets locations, governing equations and previous study of street inlet. Besides, it also presents a review on random variable and probability distribution, standard normal distribution, limit state functions and Monte Carlo Simulation.

2.2 Street Inlet

The main function of a street is to facilitate traffic movement (Guo, 2000). But, due to urbanization, stormwater that flow on a street can become a traffic obstruction (Akan and Houghtalen, 2003). Beside interrupt traffic, it also can cause accidents due to hydroplaning, skid resistance and loss of visibility from splash (Johnson and Chang, 1984). Hence, it is important for street pavement to have an effective removal of storm water as part of urban stormwater management plan (Akan and Houghtalen, 2003). Generally, street inlet is one of the urban drainage infrastructures that remove storm water from street pavement.

Function of a street inlet is to collect stormwater runoff from street pavements and discharge it into a stormwater drainage system (Akan and Houghtalen, 2003). It is essential to designed street inlet properly to avoid excess runoff which can lead to contribution of a serious problem for pedestrian and

vehicular that used the street. To design an efficient street inlet, it requires consideration on storm water runoff, gutter flow, inlet capacity and spacing (Despotovic et al., 2008).

Based on Urban Stormwater Management Manual for Malaysia, there are three major types of street inlets utilised for pavement drainage system in Malaysia:

- Grate inlet
- Curb-opening inlet
- Combination inlet, grate and curb

2.2.1 Grate Inlet

Grate inlets as shown in Figure 2.1 is an opening structure in the ditch or gutter covered by a grate and generally it loses capacity with increase in grade (Brown et al., 2013). Grates have variations of number of steel bars and spacing (Guo, 1997). Steel bars of the grate can be designed either in longitudinal or transverse direction.

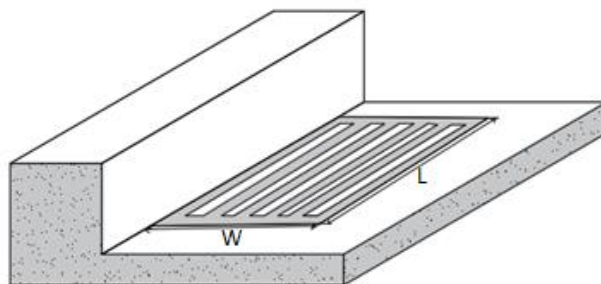


Figure 2.1: Grate inlet (Adapted & revised from Guo, 1997)

Longitudinal bar grate inlet is designed with the bars arranged parallel to the direction of flow (Figure 2.2(a)), while transverse bar grate inlet is designed with bars arranged perpendicular to the direction of flow (Figure 2.2(b)). Grate inlet with longitudinal bar to the curb and have an adequate clear length is the most efficient inlet because the water able to pass through opening without hitting a crossbar or the far side of the grate (Linsley et al, 1992). Therefore, it has high

efficiency compared to transverse grate inlet. On the other hand, longitudinal bar with wider spacing are more efficient compare to small spacing because the debris can pass through bars more easily (Brown et al., 2013).

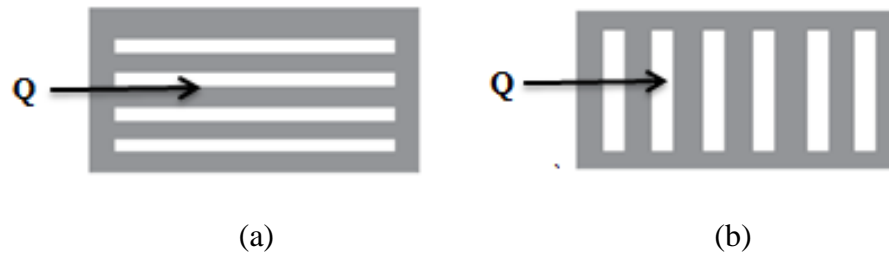


Figure 2.2: Grate inlet design with (a) longitudinal and (b) transverse grate

Basically, efficiency of a grate inlet depends on the size, amount of storm water flowing over the grate, flow velocity in the gutter and configuration of the grate (Johnson and Chang, 1984). Grate inlet efficiency was determined by the total gutter flow whereby it consists of two part which is frontal flow, and side flow. The frontal flow is the portion of the total gutter flow within the width of inlet meanwhile side flow is the flow portion outside the grate (Akan and Houghtalen, 2003).

2.2.2 Curb Opening Inlet

Curb-opening inlet or also known as kerb inlet as shown in Figure 2.3 is a vertical opening curb structure which is covered by a top slab (Brown et al., 2013). It has certain advantages compare to grate inlets whereby they are not interfered with traffic operations and tend not to clog (Akan and Houghtalen, 2003). Curb inlet efficiency highly dependent on flow depth at the curb and curb opening length (Brown et al., 2013). To have an effective performance, the flow depth must be sufficiently enough to capture the flow of water (Akan and Houghtalen, 2003).

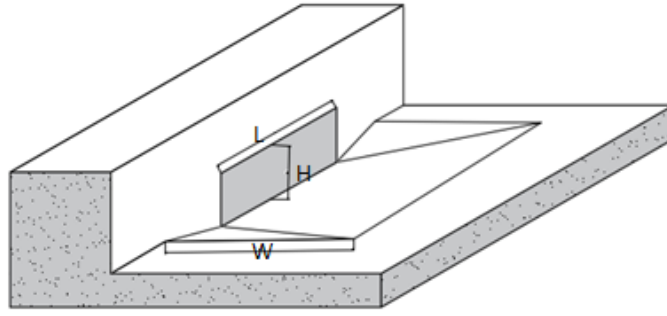


Figure 2.3: Curb opening inlet (Adapted & revised from Guo, 1997)

Curb-opening inlet can be designed to be depressed, undepressed and installed with deflectors. Based on the Hydraulic Engineering Circular No.22 (2013), depressed curb-opening inlet (Figure 2.4(b)) has higher interception compared to undepressed inlet due to the increase of water flow depth. Undepressed curb inlet (Figure 2.4(a)) performed inefficient when the street of the slopes is high because the velocity of water is high but the opening is inefficient to capture the flow. Thus, they are more suitable to be installed where the grade is low. In terms of safety, undepressed curb inlet is safer compared to grate inlet because the design does not interfere the traffic.

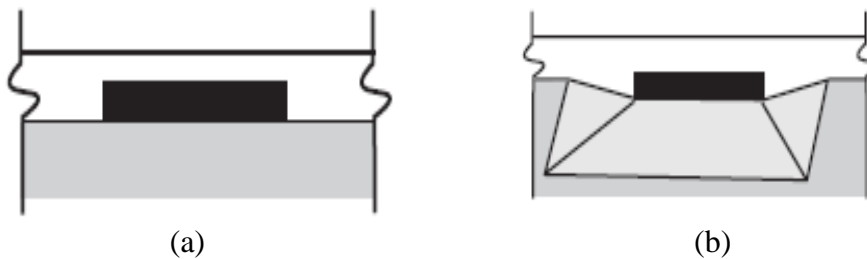


Figure 2.4: Curb-opening inlet (a) undepressed and (b) depressed

2.2.3 Combination Inlet

Combination inlet as shown in Figure 2.5 is a combination of both grate inlet and curb opening inlet placed in a side-by-side configuration and therefore it provides advantages of both (Brown et al., 2013). Usually, combination inlet is used with part of the curb opening located upstream of the grate and the interception

capacity is about the same as the grate alone either the grate and curb opening are placed side by side with equal lengths (Akan and Houghtalen, 2003).

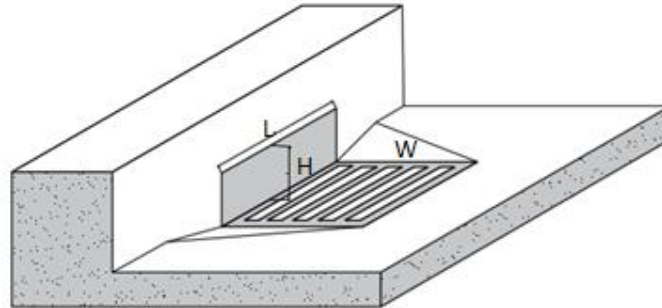


Figure 2.5: Combination inlet (Adapted & revised from Guo, 1997)

2.3 Advantages and Disadvantages of Street Inlets

For grate inlet type, they are effective in intercepting gutter flow and can perform very well over a wide range of grades. With variations of spacing and layout of steel bars, it has many types of grates design. Each design is different to suit the considerations of bicycles and pedestrians. It must be bicycle safe and foreseeable. However, the disadvantages is that it can become clogged with debris easily as shown in Figure 2.6 and lose some capacity with increasing grade.



Figure 2.6: Clogged grate inlet

Next, combination inlets are composed of inlet grates and curb openings. It should be made bicycle safe. Combination inlet has more advantages compared to curb opening and grate inlet alone. It does not clog easily and has high capacity to capture stormwater. It has high capacity because the flow interception capacity was approximated by the sum of the flow amounts intercepted by the curb opening and grate inlet (Guo, 1997). It is the most efficient inlet, but their cost to install is more expensive than others. Basically, each type of inlet has its own advantages and disadvantages and no single type of it can be considered the best (John Hopkins, 1956).

During stormwater event, water will fall from the surface of the pavement to the street gutter. For a street gutter, it has three types which are uniform gutter, curved gutter and composite gutter. Composite gutter as shown in Figure 2.7 has composite cross section parameters such as street cross slope, longitudinal slope, gutter and curb.



Gutter and curbs are to provide a barrier for the runoff to accumulate and transferred into the inlet and provide delineation. To facilitate economical construction in Malaysia, curb and gutter has a standard size. Based on MASMA (2000), by considering the vehicle and pedestrians safety, the standard curb height is 150mm.

Generally, storm water that flow on the street can be divided into two which is gutter flow and side flow. Gutter flow is the amount of flow carried within the gutter width and meanwhile term side flow is used to describe flow carried by the street. According to MASMA, street inlet in Malaysia always failed because the gutter is poorly formed or absent, inlets too widely spaced and due to poor design which is inadequate to capture the gutter flow into the street inlet.

2.5 Location of Street Inlets

Street inlet may be located either on a grade or in a sump as shown in Figure 2.8. Generally, the location of street inlet is determined by the roadway geometry. On a grade, the stormwater flows continuously and captured by the inlet. On the other hand, in a sump such as low point in a depressed location, the stormwater will accumulate at the inlet (Guo, 1997).

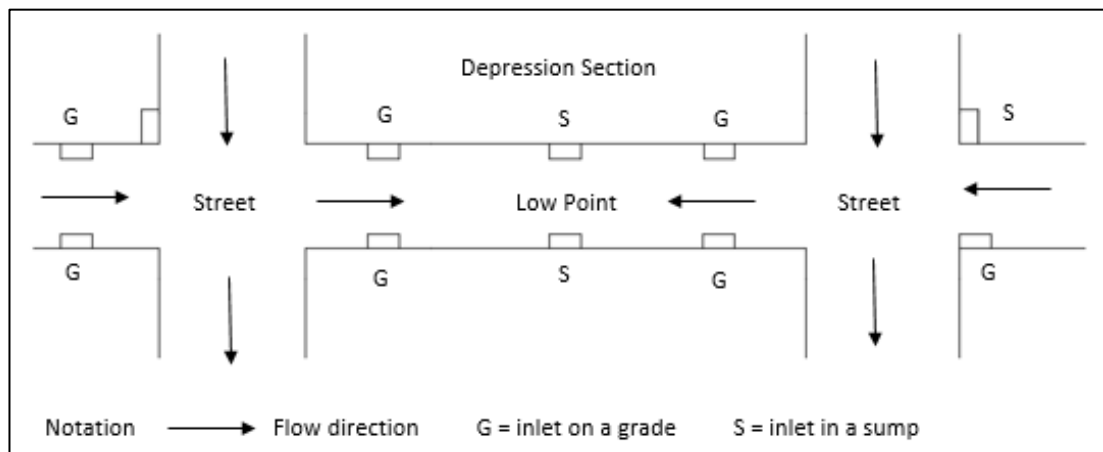


Figure 2.8: Location of Street Inlet (Adapted from Guo, 1997)

2.5.1 Grate Inlet on Grade

On a continuous grade, the ability of grate inlet to intercept flow increases when the gutter flow increases but the capture efficiency decreases. For grate inlet, the efficiencies are largely dependent on the width and length of the grate. From the dimension, it will affect the interception flow amount. To determine the interception of frontal flow whereby it passes over the grate, it needs to consider the length of grate, gutter flow and splash velocity (Guo, 1997). Splash velocity means the velocity under the grate interference.

In the design of grate inlet, when the grate has sufficient length with low velocity of the gutter flow, then the grate inlet able to intercept all the frontal flow. Meanwhile, if the grate length is insufficient or gutter flow velocity is high, a splash over will occur over the grate and only a small portion of frontal flow able to be intercepted.

According to Guo (1997), it stated that the inlet capacity increased by using multiple grate system whereby the number of inlet grates increase. In term of efficiency, grate inlet on a grade have higher efficiency in intercepting gutter flows compared to curb inlet. But, it's efficiency usually got affected or decrease when it is subjected to clogging effect by the debris. The clogging condition for on grade inlet is where clogging effect linearly proportional to the inlet length (Guo, 2006).

2.5.2 Grate Inlet in Sump

Inlets placed at low points is considered as inlets in a sump. Low points occur when street inlet located at a roadway segment whereby negative grade and positive grades joined together or at a street corner (Guo et.al, 2009). In a sump condition, clogging of inlet can lead to safety hazard for the street users especially during heavy storm water. Therefore, grate inlets are not suitable to be used in a sump due to its design which tends to clog easily. For a sump inlet, the clogging effect is linearly proportional to the inlet opening area (Guo, 2006).

At low point, when total interception is required, grate inlet will behave as either a weir or an orifice (Guo et.al, 2009). At shallow depths, storm water that flow into the sump inlets will operate like weirs and it starts to operate like an orifice as the depth of storm water increases. Changes of the water depth will cause the flow continuously changes from weir flow, through transition flow, to orifice flow as the water becomes deep enough (Guo. et.al, 2009).

2.6 Governing Equations of Street Inlets

To determine inlet efficiency, it depends on two factors which is the water depth and local street slope at the inlet. Inlet that is located in a sump can operate as a weir and also as orifice governed by the height of water depth. When water depths are low, it means it is so shallow that the inlet opening is not submerged and operates as a weir. Meanwhile, an inlet operates as an orifice when the inlet opening is fully covered by water. Between weirs and orifices, the water flow will be in transitional flow which is cannot be accurately defined due to the flow fluctuation.

2.6.1 Weir Flow

Weir as shown in Figure 2.9 is a barrier over where the water flows in an open channel. It is a structure built across a channel to raise the level of water with water flowing over it. Water that flows over the surface is called crest and overflowing sheet of water is called nappe. Weirs hydraulic structure can be sharp crested weir or broad crested weir. Sharp crested weirs are classified based on the shape of the weir crest such as rectangular weirs, triangular or also known as V-notch weir, parabolic weirs and trapezoidal weirs. Sharp crested weirs consist of vertical thin plate with a sharp edge to insure a line of contact with the flow.

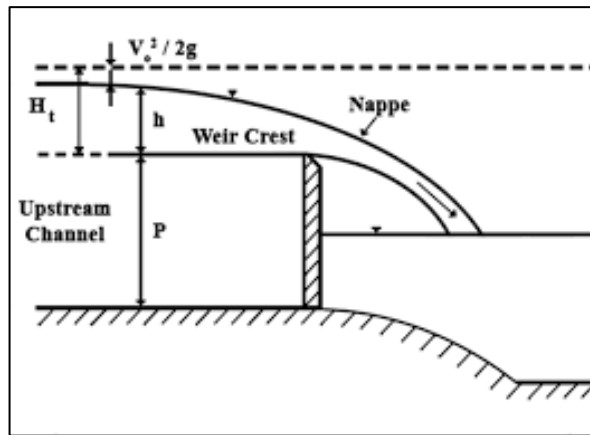
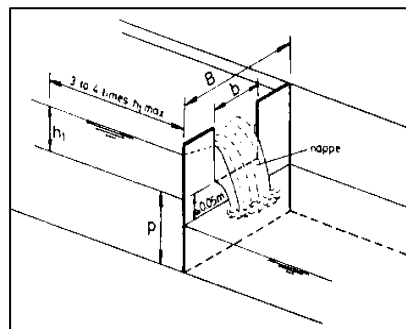
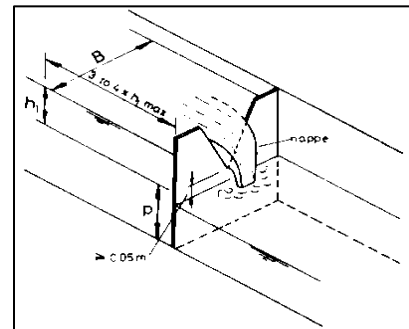


Figure 2.9: Sharp-crested weir
(Adapted from Bilhan & Emiroglu, 2016)

Among all type of weirs, as shown in Figure 2.10, rectangular weirs is the most popular because it is easy to construct. But, a triangular weir or also known as V-notch weir is more useful than rectangular because they have a higher degree of accuracy over a wide range of flows. Generally, weirs are used to measure or control hydraulic devices. Due to that, weirs concept was applied to measure and analyse the efficiency of a street inlet.



(a)



(b)

Figure 2.10: Types of weir (a) rectangular weir and (b) triangular weir (Adapted from Chapallaz et al., 1992)

The capacity of grate inlet under weir control is:

$$Q_w = C_w P d^{1.5} \quad (2.1)$$

Where C_w is the weir coefficient, 3.0 for ft^3/s and 1.66 for m^3/s , P is the grate perimeter disregarding both bars and the curb side and d is the depth of water over the inlet.

2.6.2 Orifice flow

Orifice flow is a flow whereby the water completely submerged the opening of an inlet. The capacity of grate inlet under orifice control is:

$$Q_i = C_o A (2gd)^{0.5} \quad (2.2)$$

Where C_o is the orifice coefficient, 0.67, A is the clear opening area of the grate, g is the acceleration due to gravity and d is the depth of water over the inlet.

2.6.3 Froude Number

Froude number (Fr) is a dimensionless quantity that represents the ratio of inertial to gravity forces (Chaudry, 2008). It also represents different flow regimes in open channel flow. In street inlet, Gomez and Russo (2009) stated that dimensionless quantity such as Froude number of the approaching flow highly linked with the surface roughness, discharge and the street geometry. Froude number can be defined as

$$F = \frac{v}{\sqrt{gy}} \quad (2.3)$$

Where v is the flow velocity upstream the grate and y is the depth of the flow (Russo et al, 2013). Flow parameters such as Froude number are used to study hydraulic efficiencies of the street inlet.

2.7 Studies of Street Inlets

By using inlet design used in Singapore, a study conducted by Veerapan and Le (2016) on hydraulic efficiency of street inlets under clogging effect found that the performance of longitudinal grate inlets is higher than lateral grate inlets. It intercepts 2.5% more flow than lateral grate. Under a 100% clogging effect, the study shows that the inlet design with lateral bars extended over curb opening has higher efficiencies more than 50% compare to longitudinal and lateral grate inlets.

Next, it was found that inlet capacity are governed by the rate of water removal from the gutter and amount of water that inlet can receive and enter into the storm water drainage (Gomez et al., 2014).

An experimental study done by Guo and MacKenzie (2012) on hydraulic efficiency of selected street inlets under clogging effect has found that combination inlet has 3% higher hydraulic efficiency compare to grate inlet and 12% higher when compare with curb inlet. Besides, they also found that for sump inlet, the flow interception capacity is determined by weir or orifice flow and combination inlet using a bar grate has a higher reduction factor compare to using a vane grate.

Brendan et al. (2009) had also conducted experimental studies of selected street inlet (grate, vane grate and curb opening inlet). The results show that on a grade, vane grate inlet is the most efficient with the highest hydraulic efficiencies followed by bar grate inlet and curb opening inlet. When it is tested in the sump, the results found that grate inlet performed better than vane grate inlet and followed by curb opening inlet.

On top of that, from their study, it was found that for on grade, the highest hydraulic efficiency obtains at the lowest flow velocity with influenced by the cross and longitudinal slope. The efficiency increases when the length of the inlet increase and efficiency decrease when the cross slope and longitudinal slope decrease or lower as the velocity increases.

Another experimental study was done by Bruce et al. (1999) on hydraulic performance of several curbs and gutter inlets (concrete gutter inlet, Type B gutter inlet, Type 12 combination inlet and Type 22 curb inlet). From the experiment, they have concluded the concrete gutter inlet, Type B gutter inlet, Type 12 combination inlet have similar hydraulic performance characteristics. They also have concluded that the entire inlet tested performs slightly better on a steep grade compare to mild grades. Type 12 combination and Type B inlet was found to have higher efficiency compare to Type 22 curb inlet.

Next, from previous study carried by Gomez and Russo (2009) on some transverse grate design with various widths, they have obtained experimental equations that relate hydraulic efficiency of inlet to some relevant parameter such as hydraulic depth and Froude number.

$$E = \alpha \left[F \left(\frac{y}{L} \right)^{0.812} \right] + \beta \quad (2.4)$$

Where by L is the length of the minimum rectangle including the void area in the flow direction, y/L is the normalized water depth related to L, F is Froude number and α and β are exclusive whereby it depends on the geometric characteristics of the grates. From the equation, Gomez and Russo have suggested to use it as a first approach in surface drainage system design. Besides, Gomez and Russo also stated that for dimensionless quantity such as hydraulic efficiency must only depend on the grate geometry and the Froude number of the approaching flow.

According to Guo et al. (2009), for sump inlet performance, the capacity increases with respect to the water depth from weir flow to orifice flow. When comparing the experimental results under no clogging effect with HEC 22, it is found that HEC 22 had overestimated the capacities for both combination and grate inlet. Meanwhile for curb opening inlet, HEC 22 underestimates it for deep water depths and overestimates it for shallow water depths.

2.8 Random Variable and Probability Distribution

For representing an event in analytical form, the value of a random variable is used to define within a range of possible values. If X is defined as a random variable, then $X = x$, $X < x$ or $X > x$ represents an event, where $(a < x < b)$ is the range of possible values of X (Ang and Tang, 2007). In random variable, it consists of two types which are discrete and continuous random variable.

X is discrete random variables if only values of x are countable finite or infinite number of distinct values or have positive probabilities. For discrete, its probability distribution is described by its probability mass function (PMF). Meanwhile, X is continuous random variables if probability defined for all values of x . For continuous, its probability distribution is described as probability density function (PDF).

2.9 Standard Normal Distribution

There are many types of distribution function and one of the most widely used was Gaussian probability distribution or also well known as standard normal distribution. Normal distribution is denoted as $N(0, 1)$ whereby the parameters $\mu=0$ and $\sigma=1$. Its probability density function (PDF) is accordingly:

$$f_X(x) = \frac{1}{\sqrt{2\pi}} e^{-\frac{1}{2}x^2} \quad (2.5)$$

Standard deviation is used to describe the dispersion or scatterness of the data values. In normal distribution, it is used to control the spread of the data distribution. Larger value of standard deviation will give a wider and flatter normal distribution because the data is spread out around the mean. Meanwhile, smaller value of standard deviation will give the opposite. The normal distribution will be taller because the data is tightly gathered around the mean.

Standard normal distribution as shown in Figure 2.11 also called as bell curve. The total area under the curve is equal to 1 and has the mean, mode and median which are all equal. The bell curve is having a symmetrical curve at the center. A symmetrical curve will have half of the values to the positive side and the other half to the negative side.

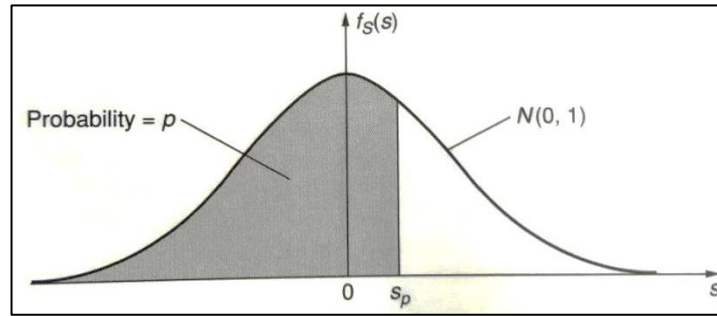


Figure 2.11: Standard Normal Distribution Function
(Adapted from Ang & Tang, 2007)

2.10 Limit State Function, Strength and Load

“A limit state of a structure entails its loads at which the structure is just on the verge of not satisfying the intended function. The structural performance maybe treated in probabilistic terms by means of limit state function, which is the most important uncertainties – the basic random variables. Limit state function is the boundary between reliability and unreliability of the structure concerned (Chen, 2015)”.

In reliability analysis, limit state function or also known as failure function needs to be defined. The reliability of this research is concerned with hydraulic failure of grate inlet. Grate inlet is considered as hydraulic failure when it fails to deliver flow fully into the urban drainage system. In this research, the function expresses the criterion of failure in grate inlet design. Generally, limit state function represented with letter Z and addresses as below:

$$Z = R - S \quad (2.6)$$

Where, R represents strength or the resistance to failure and S represents load or known as that which is conducive to failure (Mustaffa, 2011). In hydraulic design, higher R value is more reliable than lower R (Gui et al., 1998). Based on the function, it can be concluded that a system will go under failure condition when the function gives negative value meanwhile a system is stable when it gives positive value.

$Z < 0$, under designed

$Z > 0$, overdesigned

$Z = 0$, optimized design

From the limit state function, probability of failure can be described as,

$$P_f = P_r(Z \leq 0) = P_r(R \geq S) \quad (2.7)$$

In terms of reliability, it can be express as,

$$P_r(Z > 0) = 1 - P_f \quad (2.8)$$

2.11 Monte Carlo Simulation

In most of the practical engineering situations, problem involves maybe complicated and not amenable to analytic solutions. Therefore, in dealing with a complex probabilistic problem, a practical method to find the solution is by using Monte Carlo Simulation (MCS) which has wide applicability to solve probability problem (Ang and Tang 2007). This computerized mathematical method allows us to solve problem for risk in decision making and quantitative analysis.

For reliability analysis, MCS is applied by randomly generate the sampling values of random vector, X from a distribution function (Tran, 2016). MCS works by substitute a range of values (probability distribution function) to generate models of possible results. Then, each time a different set of random values is used, the results will be calculated over and over. The repetition could involve thousands, or tens of thousand times depend on the number of uncertainties before it is fully complete to form a simulation with a distribution of possible outcome values.

In this research, a normal distribution is used for each variable. Therefore, for a normal distribution, the random number sampling and transformation is expressed as follows:

$$X = \sigma R + \mu \quad (2.9)$$

Where σ = mean and μ = standard deviation of random variable and R = random number generated from the normal distribution (Lian et al., 2003)

When computer run and generates a random sample for each variable each time, function Z is also computed. From the total number of runs, the risk or probability of failure of a system is determined by the probability of negative Z values obtained out of the total number runs.

CHAPTER 3

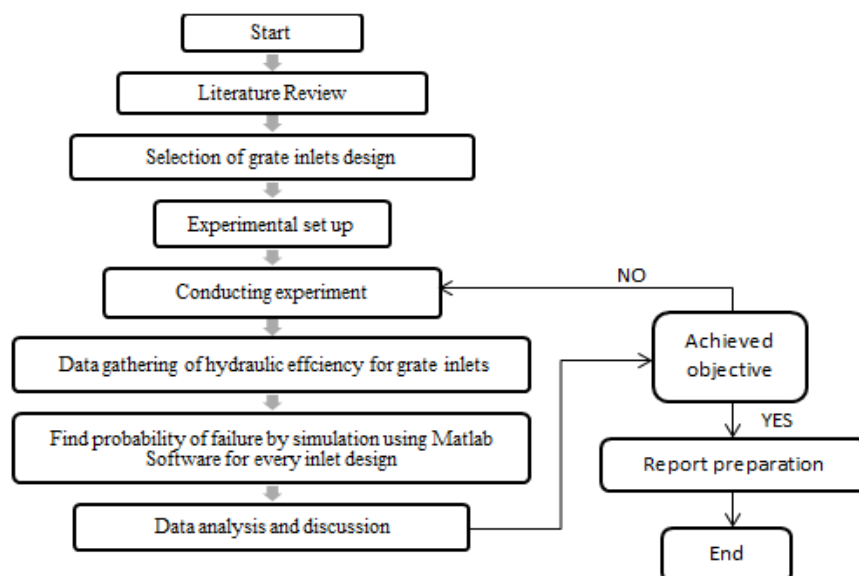
RESEARCH METHODOLOGY

3.1 Introduction

Throughout this chapter, it will give an overview on the research methodology used in order to achieve the objective of this research. This chapter presents the flowchart, Gantt chart, experiment parameters and methodology. The aim of conducting these experimental studies is to determine the hydraulic efficiencies of grate inlet by using full scale roadway flume prototype and able to conduct an analysis on reliability of street inlet based on data obtained from experiments.

3.2 Research Flow

The flow of the research is displayed below:



3.3 Selection of Grate Inlet Designs

Three types of grate inlet design as shown in Figure 3.1 were selected to be tested in this experimentation. These grate designs were used to study and compare their efficiency to capture water into the inlet. All grate inlets were designed with the same width and different length and bar configuration (Figure 3.2). Two grate inlets were in transverse and the other one was in longitudinal. By referring to Table 3.1, the width of the entire grate inlets remained the same while the length was difference for transverse grate inlets.

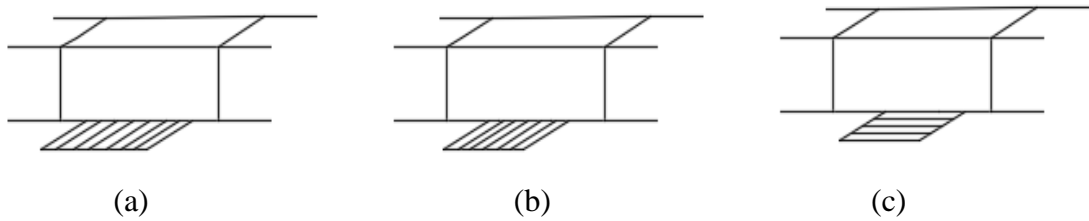


Figure 3.1: Three different design of (a) grate inlet 1, (b) grate inlet 2 and (c) grate inlet 3

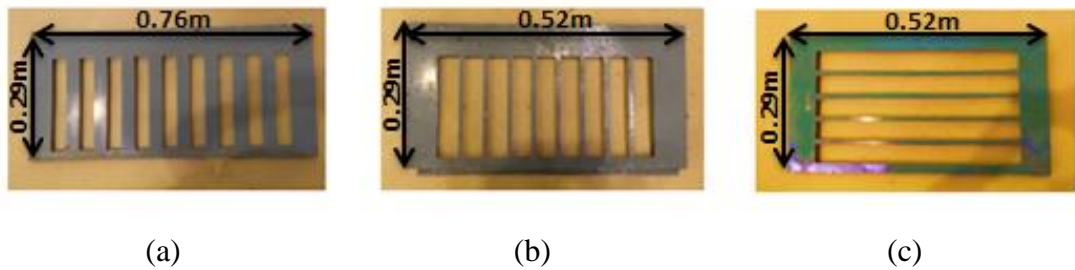


Figure 3.2: Bar configurations of (a) grate inlet 1, (b) grate inlet 2 and (c) grate inlet 3

Table 3.1: Grate inlets specifications

Grate inlet specifications	Grate Inlet 1	Grate Inlet 2	Grate Inlet 3
Grate Length (m)	0.29	0.29	0.29
Grate Width (m)	0.76	0.52	0.52
Area of opening (m^2)	7.56	7.20	8.80
Bar configuration	Transverse	Transverse	Longitudinal

3.4 Experimental Set Up

3.4.1 Half Roadway Flume

Experimental set up of the existing roadway flume was performed at Block J of Universiti Teknologi PETRONAS. The model as shown in Figure 3.3 consists of tank that supplies and produces sheet flows, a flume with street inlet, several flow-measurement devices and two tanks to capture bypass and intercepted flows. The roadway flume was constructed with slope parallel to the direction of the road, S_o designed as 0.5%, slope perpendicular to the direction of the road, S_x designed as 2.5% and slope perpendicular to the gutter flow, S_w designed as 4%. It is a typical design used in Malaysia based on JKR standard.

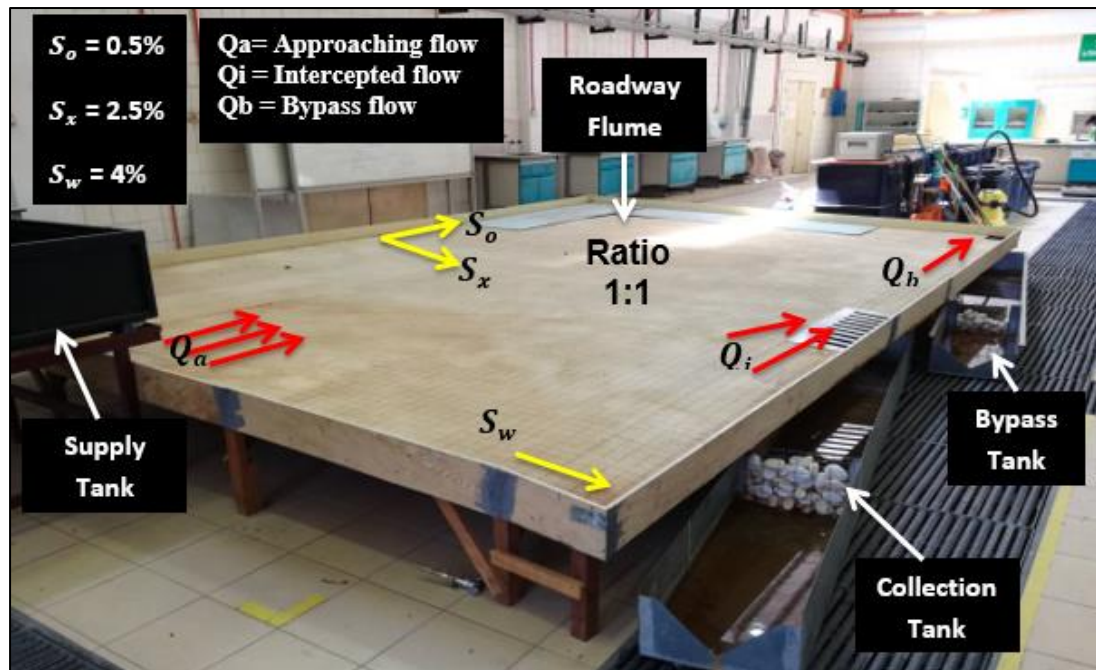


Figure 3.3: Half roadway flume set up

3.4.2 Types of Tank

Three types of tank were used, namely supply tank, collection tank and bypass tank, as shown in Figure 3.4. There are three types of weir used to measure the flow.

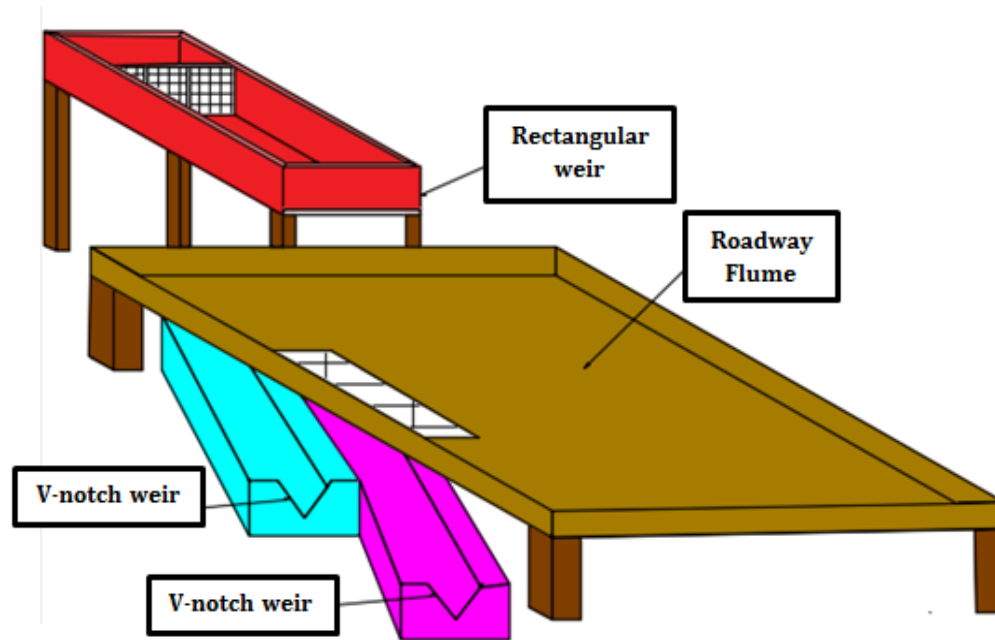


Figure 3.4: Types of weir

Supply Tank

For the supply tank, a rectangular weir was built in it, as shown in Figure 3.5 to collect water and produce approaching sheet flows on to the roadway flume.

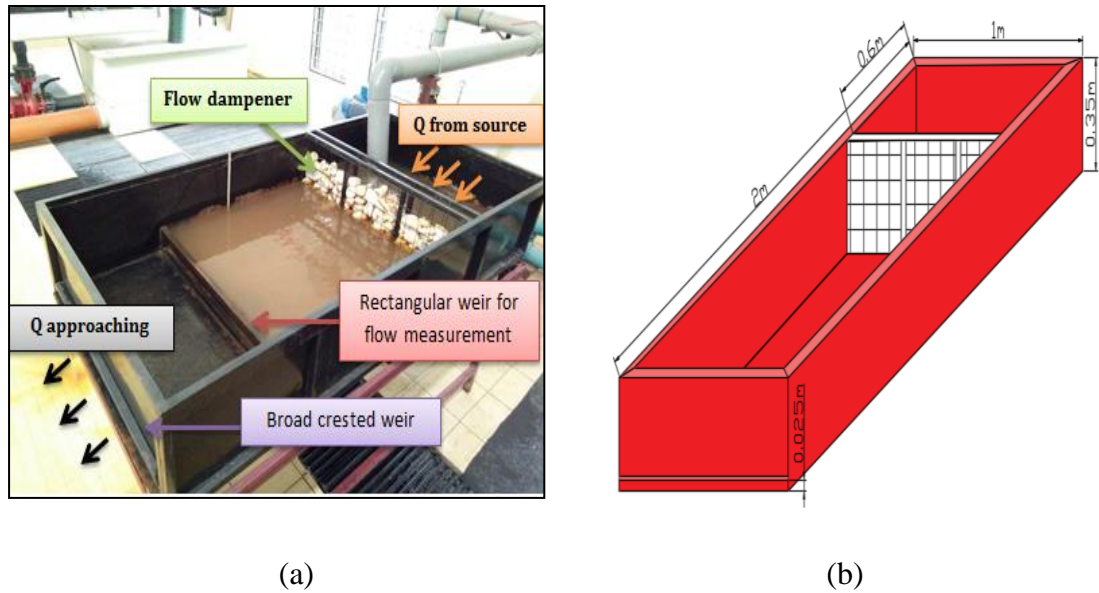


Figure 3.5: (a) Actual and (b) 3D drawing of rectangular weir

Bypass Tank and Collection Tank

Meanwhile, to measure the intercepted and bypass flows, the bypass and collection tanks used triangular weir or also known as V notch weir as shown in Figure 3.6.

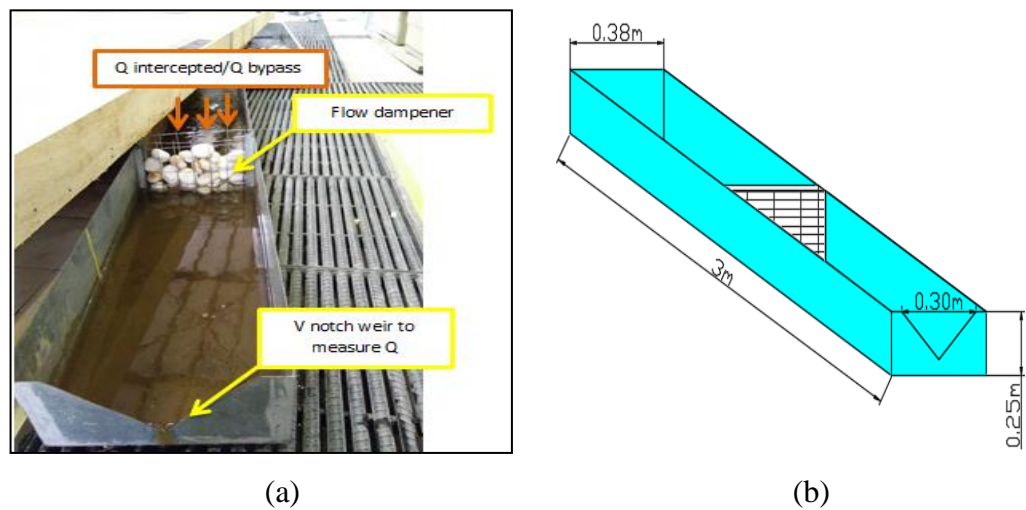


Figure 3.6: (a) Actual and (b) 3D drawing of V-notch Weir

3.4.3 Flows of Experiments

Figure 3.7, shows a sketch of the plan view of the full-scale half roadway flume when the water flows on the flume.

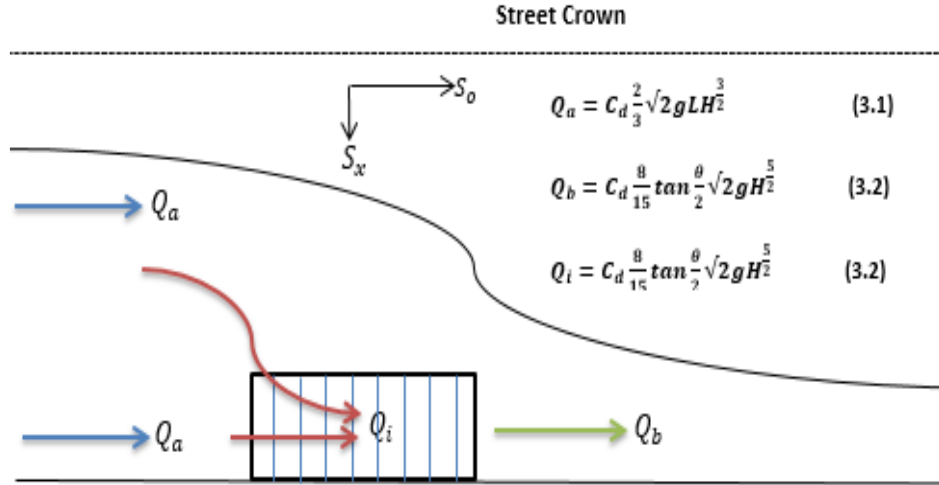


Figure 3.7: Sketch of the plan view of the half roadway flume

In this experiment, the source of water was supplied from a supply tank using pumping system facilities. From the supply tank, it produced an approaching flow, Q_a in the form of sheet flow entering the roadway flume. Sheet flow is produced to avoid concentrating flows. The approaching flow was then calculated using Equation (3.1).

$$Q_a = C_d \frac{2}{3} \sqrt{2g} L H^{\frac{3}{2}} \quad (3.1)$$

Where

C_d = Discharge coefficient

g = Gravity (m/s^2)

L = Width of weir (m)

H = Head of water above the crest (m)

Next, the approaching flow flowed and intercepted by the installed grate inlet. As the water being intercepted by the inlet, the intercepted flow, Q_i was transferred

in the collection tank. At the same time, some of the approaching flows would become bypass flows, Q_b . The bypass flow was then transferred into the bypass tank. Head of water in both tank was then measured by a triangular V-notch weir and calculated by using Equation (3.2), At the same time, head of water over the grate inlet were also measured.

$$Q_i = Q_b = C_d \frac{8}{15} \tan \frac{\theta}{2} \sqrt{2g} H^{\frac{5}{2}} \quad (3.2)$$

Finally, after obtained values of approaching, intercepted and bypass flows, Equation (3.3) was used to calculate the efficiency of the inlet.

$$\text{Efficiency, } \eta = \frac{Q_i}{Q_a} \times 100\% = \frac{Q_a - Q_b}{Q_a} \times 100\% \quad (3.3)$$

By using the same inlet design, the experiment was repeated by varying the approaching flow values from minimum to maximum flows. Lastly, the whole experiment was repeated using another type of inlet. The summary of the whole experiment is displayed in the flow chart given below (Figure 3.8).

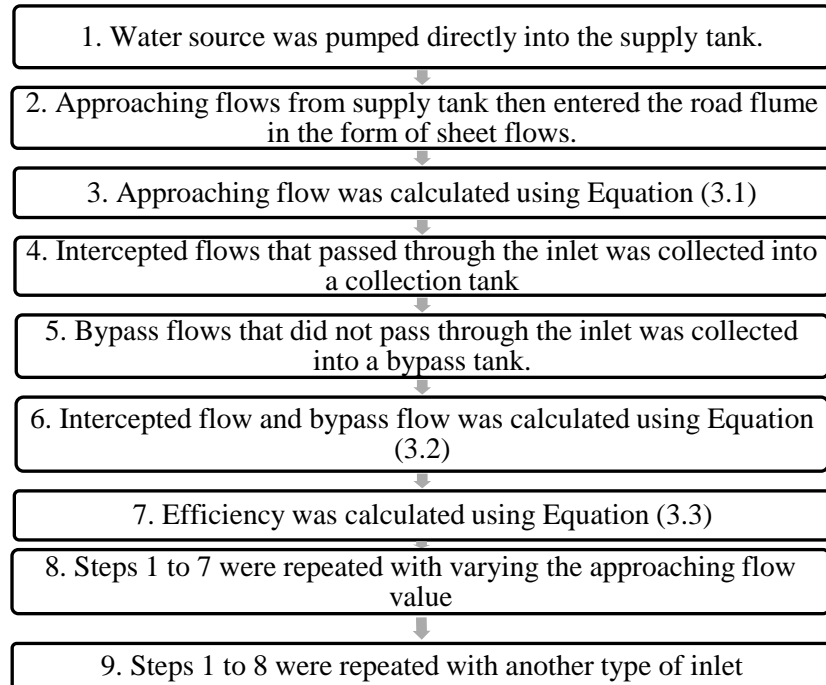


Figure 3.8: Summary of the experiment

3.5 Development of Limit State Function

In reliability analysis, it involves computing the probability of failure with a given limit state function. For this research, the limit state function was expressed as,

$$Z = Q_{i(theory)} - Q_{i(measured)} \quad (3.4)$$

From the development of this limit state function, by using the same concept of Equation (2.6), resistance of the grate inlet system is described by the theoretical intercepted flow, $Q_{i(theory)}$. The $Q_{i(theory)}$ was obtained by applying Equation (2.1) and it shows that theoretically at certain value of opening, it will have certain values of capability to intercept the approaching flows into the inlet. Meanwhile the load, was defined as measured intercepted flow, $Q_{i(measured)}$. Triangular weir equation, Equation (3.2) was applied to measure and obtain the measured intercepted flow, $Q_{i(measured)}$ during the experiment.

By using the limit state function, reliability analysis of grate inlets can be further studied. A probabilistic approach was used to determine the probability of failure (PoF) of grate inlets. By using the approach, there was four random variables involved. For random variable d and h, the mean and standard deviation were in the range as shown in Table 3.2 and Monte Carlo technique was applied for simulation to obtain the PoF.

Table 3.2: Descriptive statistics of failure of grate inlets

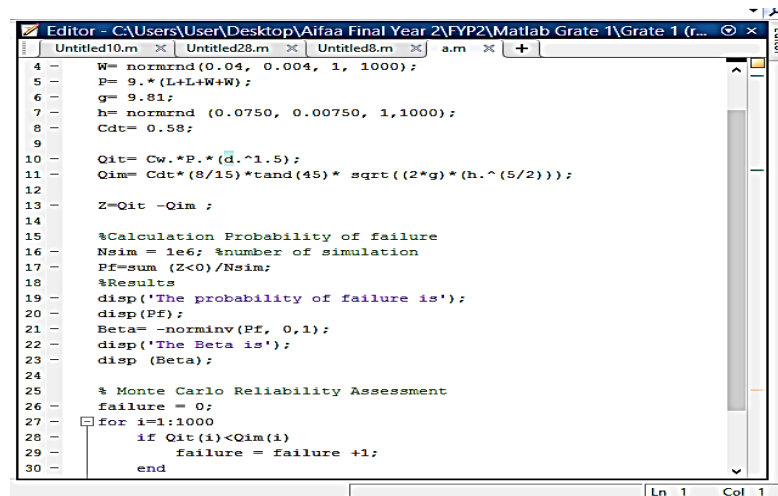
Variables			Distribution	Mean	Standard deviation
Symbol	Description	Unit			
d	Water depth over inlet	m	Normal distribution	0.015 - 0.064	0.0577 - 0.1000
L	Length	m	Normal distribution	0.290	0.029
W	Width	m	Normal distribution	0.760	0.076
h	Head water above crest	m	Normal distribution	0.034 - 0.145	0.0034 - 0.0145

3.6 Simulation of Limit State Function (LSF) Model

The performance of street inlet is uncertain and therefore reliability analysis is used to measure the reliability of the inlet performance. In this study, it examined the failure of several typical inlets in Malaysia when the approaching flow or incoming flow exceeds the capacity of the inlet to intercept the flow. The probability of failure of tested inlet is presented using Monte Carlo Simulation through MATLAB Software. In practice, the reliability model can be used to find the reliability of typical inlet and to help improving the designs of the inlet.

MATLAB (Matrix Laboratory) is a software that enables the user to solve variety of technical computing problems such as algorithm development, mathematical modelling, system design and simulation, data analysis and others. In this research, Monte Carlo simulation was used to see how a limit state function as shown in Equation (3.4) responds to randomly generated inputs by using MATLAB. By using this programming language software, probabilistic calculation for probability of failure of street inlets was able to determine.

To start the simulation, a code must be developed and written in the Script Editor as shown in Figure 3.9. All the variables such as parameter, equation and limit state function involved were written in the script. Every code for each line in the script is a useful command and must end with a semi colon.



```
4 - W= normrnd(0.04, 0.004, 1, 1000);
5 - P= 9.*(L+L+W+W);
6 - g= 9.81;
7 - h= normrnd(0.0750, 0.00750, 1,1000);
8 - Cdt= 0.58;
9 -
10 - Qit= Cw.*P.*(d.^1.5);
11 - Qim= Cdt*(8/15)*tand(45)* sqrt((2*g)*(h.^(5/2)));
12 -
13 - Z=Qit -Qim ;
14 -
15 - %Calculation Probability of failure
16 - Nsim = 1e6; %number of simulation
17 - Pf=sum (Z<0)/Nsim;
18 - %Results
19 - disp('The probability of failure is');
20 - disp(Pf);
21 - Beta= -norminv(Pf, 0,1);
22 - disp('The Beta is');
23 - disp (Beta);
24 -
25 - % Monte Carlo Reliability Assessment
26 - failure = 0;
27 - for i=1:1000
28 -     if Qit(i)<Qim(i)
29 -         failure = failure +1;
30 -     end
```

Figure 3.9: Code in the script editor

Next, after all variables have been defined, on the Editor tab, click the Run button as shown in Figure 3.10 to complete the simulation

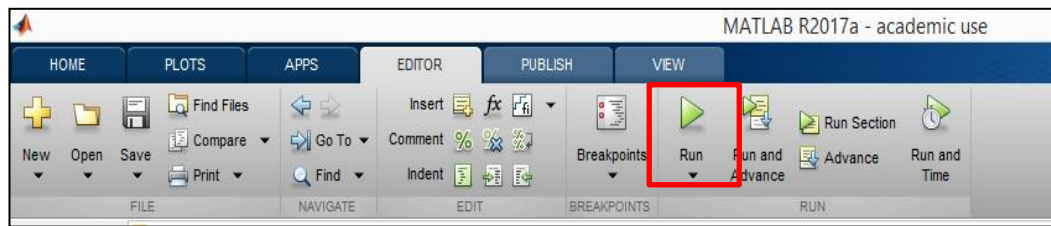


Figure 3.10: Run the program

After running the program, as shown in Figure 3.11, the Command window will display the value of probability of failure of the simulated grate inlet from Equation (3.4).

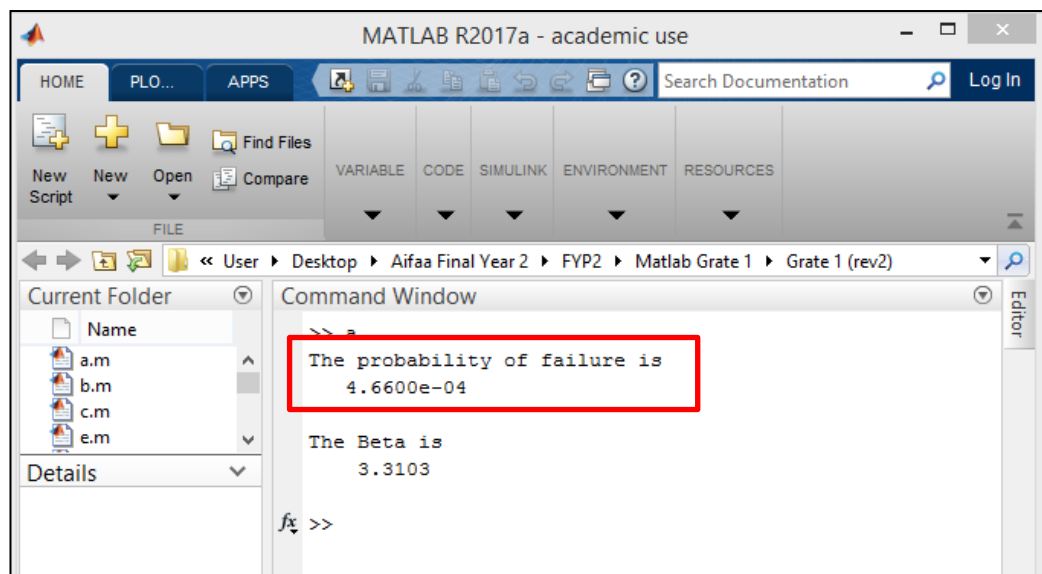


Figure 3.11: Probability of failure of grate inlet simulation

CHAPTER 4

RESULTS AND DISCUSSION

4.1 Introduction

This section describes the results and findings obtained from the experimental studies conducted on three different grate inlet designs. A graph of efficiency of grate inlets and three graphs of probability of failure were plotted and discussed in this section. Besides, observations from the experiments were also illustrated and discussed thoroughly.

4.2 Efficiency of Grate Inlets

As previously explained, the approaching flow of the model was measured by using rectangular weir and the intercepted and bypass flow was measured using V notch weir. The approaching flows were then calculated using Equation (3.1), while the intercepted and bypass flow were calculated using Equation (3.2). Equation (3.3) were used to calculate the efficiency of three different grate inlets.

Based on the result obtained in Table A.1, it was found that at approaching flows less than $0.0011\text{m}^3/\text{s}$, all inlets showed efficiency above 90%. Supposedly, all approaching flow below than $0.0011\text{m}^3/\text{s}$ that was fully intercepted should give a 100% efficiency, but due to roughness of the roadway flume some of the approaching flow was stagnant or remained on the roadway flume causing the losses.

Table A.1 also shows that, at the lowest approaching flow of $0.003\text{m}^3/\text{s}$, grate inlet 1 and grate inlet 3 obtained 100% efficiency meanwhile grate inlet 2 only obtained 97%. On top of that, at maximum flow at $0.0126\text{ m}^3/\text{s}$, it shows that grate inlet 3 gave higher efficiency with 66% while grate inlet 1 gave 62% followed by grate inlet 2 with 60%. From the results, it was clearly shown that grate inlet 3 has the highest efficiency accompanied by grate inlet 1 and lastly grate inlet 2. Grate inlet 3 captured more flow and perform better than the others because the bar configuration in longitudinal can intercept more flow than transverse.

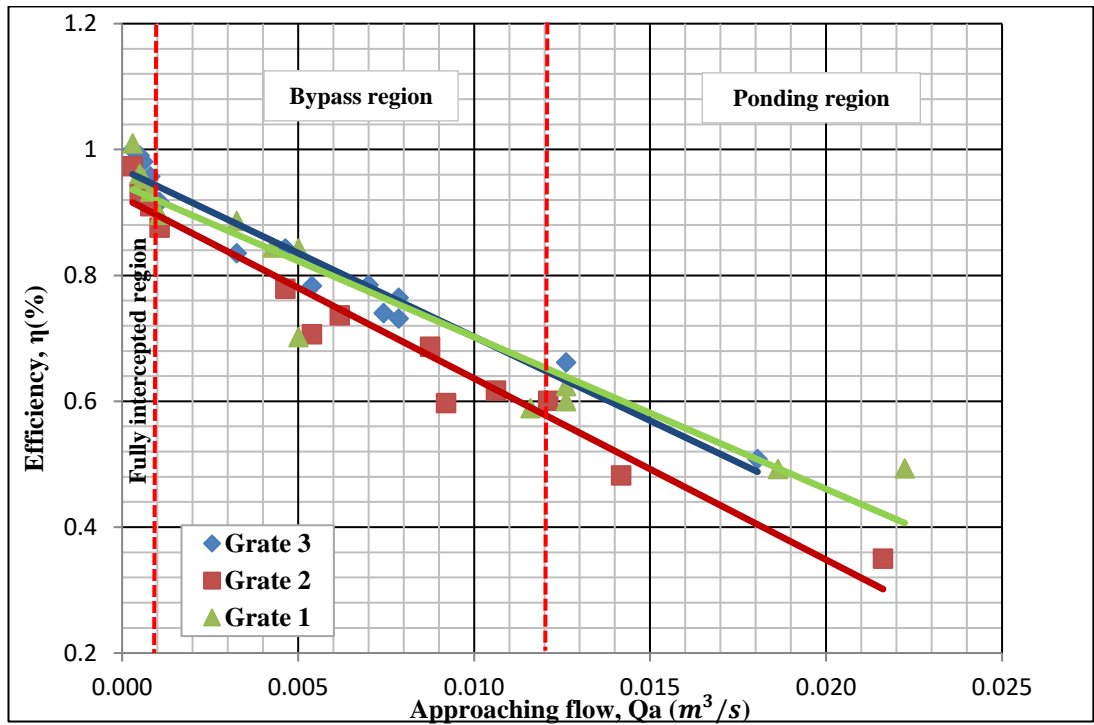


Figure 4.1: Graph of efficiency, η against approaching flow, Q_a

For illustration purposes, trend lines are fitted based on the data obtained from Table A.1 as shown in Figure 4.1. Each trend line illustrates the efficiency behaviour. Approaching flow was chosen as the variable because it has the most significant effect on the inlet efficiency.

Based on the figure, for the approaching flows less than $0.0011\text{m}^3/\text{s}$, the flows were categorized into fully intercepted region, meanwhile flows that ranging from $0.0011\text{m}^3/\text{s}$ to $0.012\text{m}^3/\text{s}$, the flows were categorized into bypass region. All incoming flows were unable to be fully intercepted and some part of the flows

become bypass flows. This is because of the velocity of the flow was high, making some amount of the water going straight to the bypass region. Meanwhile, when the flows were greater than $0.012m^3/s$, flows were fall into ponding region. When ponding occurred, it was observed that the spread of water on the roadway flume became wider. It was found that at high velocities, most flows accumulated at the bypass region and at the same time backwater taken place at the inlets. Due to the backwater effect, it has caused errors in taking the actual measurements of the intercepted and bypass flow.

From Figure 4.1, it also showed that when approaching flows increased, the efficiency of grate inlet decreased. This was because when approaching flow continues to increase, the amounts of water need to be captured and intercepted were also increased. Due to the design of the grate inlet itself, it might have limitations in its ability to intercept the flows. When it reaches the limit, bypass and ponding happened and thus the efficiency decreased. From the figure, the highest efficiency among the three grate inlets was found to be grate inlet 3 followed by grate inlet 2 and grate inlet 1. Grate inlet 3 is the highest because the bars were arranged longitudinally.

Longitudinal grate can intercept more flow because it is parallel with the approaching flow and have less occurrence of splash because the flow can intercept without hitting the crossbar or the far side of the grate (Linsley et al, 1992). From the previous studies of grate inlets by other researchers, it was stated that longitudinal grate has higher efficiency than transverse. From the experiments conducted, it was proven that longitudinal grate inlet 3 performed better than the transverse grate inlet 1 and 2. From Figure 4.1, could be seen that the efficiency of grate inlet 3 and grate inlet 1 did not differ so much and at $0.01m^3/s$, both grates were having the same efficiencies of 70% because grate 1 has larger area of grate which make it able to perform as good as grate 3. But when it is grate inlet 3 compared with grate inlet 2, which have the same length and width, the efficiencies difference was larger which proved that longitudinal grate has higher efficiency than the transverse grate.

Lastly, based on the results, grate inlet 1 performed better than grate inlet 2. This is because, transverse bars of grate inlet 1 has longer length dimensions which

increased the area of the opening and allowed more water to be intercepted into the inlet. Therefore, it can be concluded that the longer the length of the grate, the higher the efficiency.

4.3 Probability of Failure of Grate Inlets

For reliability analysis, by using limit state function given by Equation (3.4), the probability of failure (PoF) was computed by using MATLAB software and were simulated using Monte Carlo simulation technique. The PoF was then relate to three governing variables namely approaching flow, efficiency and Froude number as shown in Table A.2 to Table A.4 to understand the performance of each grate inlet. In Table A.4, only nine readings were recorded due to some error in conducting the experiment.

Based on the results in Table A.2, Table A.3 and Table A.4, it can be concluded that, grate inlet 2 has the highest probability of failure as compared to others because of transverse bar configurations and shorter length of the grate. Besides, it is also found that when the approaching flow increased, the probability of failure also increases. For illustration purposes and to understand the reliability of each grate inlet designs tested, three graphs of probability of failure which was against approaching flow, efficiency and Froude number were produced.

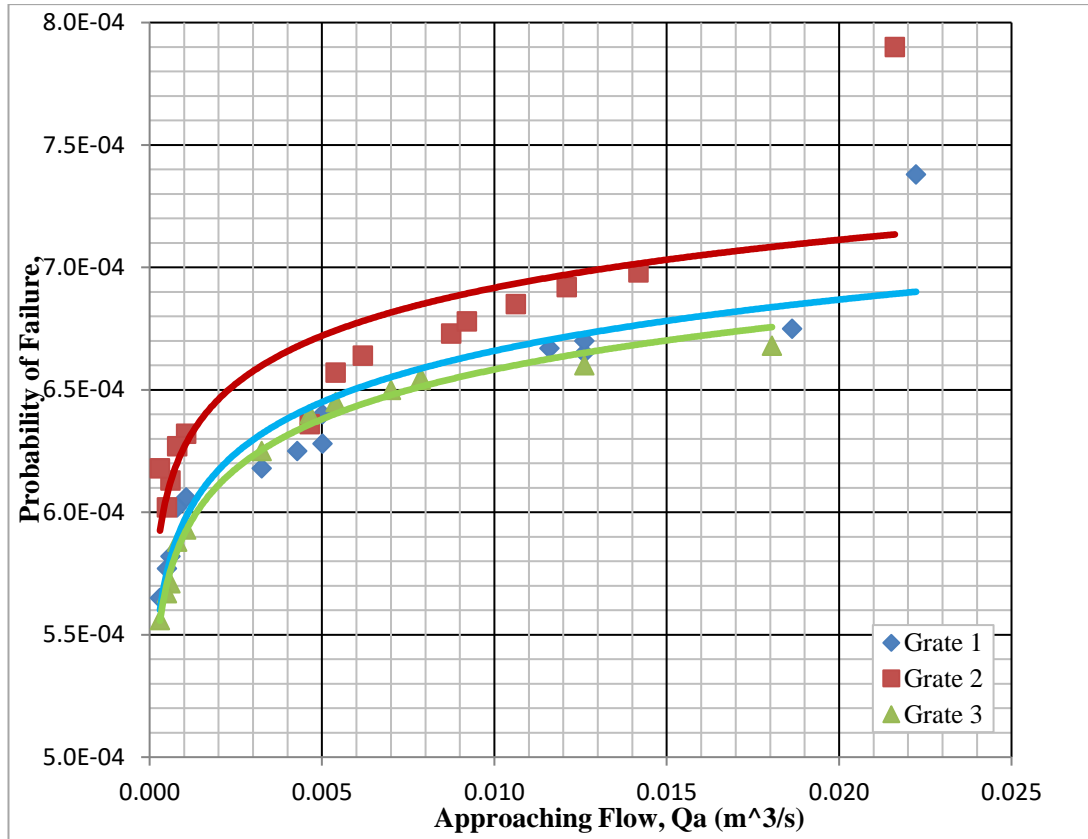


Figure 4.2: Graph of probability of failure against approaching flow

A total of 1000 trials were made at each point to plot the curves in Figure 4.2. An increase in approaching flow would likely to increase the probability of failure, particularly when the approaching flows were greater than $0.0011m^3/s$ where the certain amount of water travel at higher velocities. Figure 4.2 shows that at $0.01 m^3/s$, PoF for the grate 1, grate 2 and grate 3 were 0.00067, 0.00069 and 0.00066 respectively.

Grate inlet 2 appeared to have the highest probability of failure because of its transverse bar design. Transverse grate inlet 2 tend to fail in intercepting most of the approaching flows as compared to transverse grate inlet 2 with longer length and longitudinal grate inlet 3. Moreover, it was also clearly showed in Figure 4.2 that there was a larger gap of probability of failure between grate inlet 2 and the others which means transverse grate inlet are having the lowest reliability and performance as compared to others. Meanwhile, the PoF between grate 1 and grate 3 were not too much different because their designs having similar capability in intercepting the

approaching flows. Therefore, in selecting the design of grate inlets, longitudinal grate inlet was more preferable in order to capture the approaching flow efficiently.

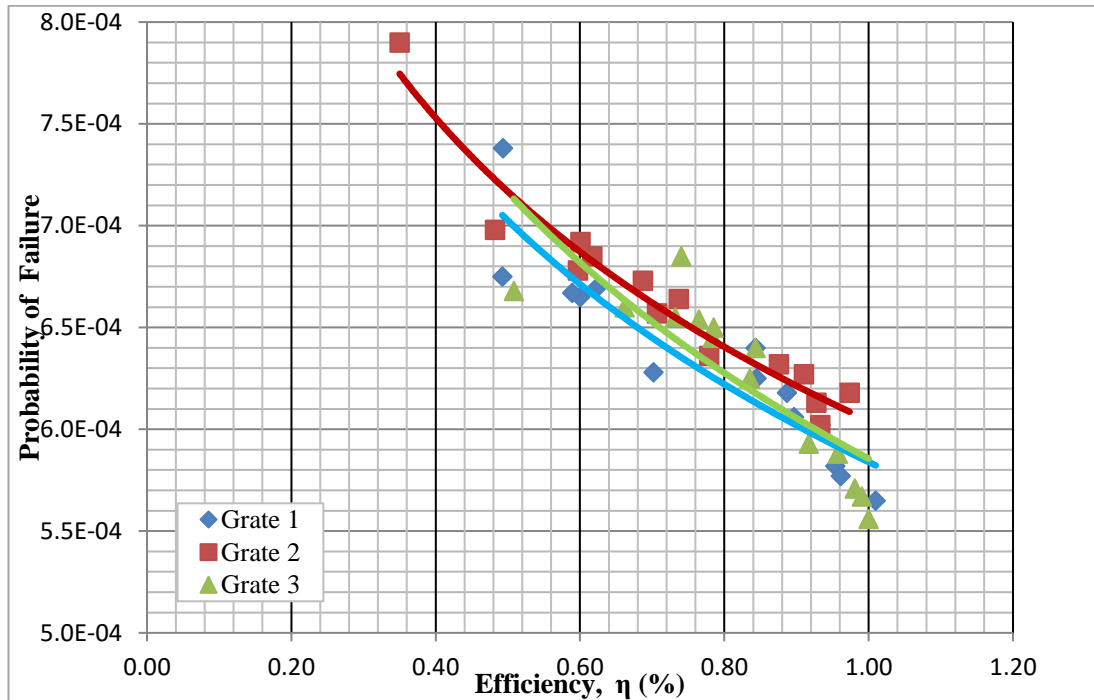


Figure 4.3: Graph of probability of failure against efficiency

Figure 4.3 demonstrates the probability of failure against efficiency of different grate inlets. Efficiency of grate inlets depends on the capability of the grate inlet to intercept the approaching flow as much as it could. Based on the graph plotted, it shows a downward trend for each design. When efficiency of the grate inlets increased, the probability of failure decreased. At 60% efficiency, grate inlet 3 has PoF of 0.00067 and when efficiency increased to 80%, the PoF decreased to 0.00062.

Grate inlet 3 was found to have the highest efficiency which means it is the most reliable compared to others designs tested. However, Figure 4.3 shows a slightly difference trend from Figure 4.1. Although grate inlet 3 has the highest efficiency against approaching flow, when it was compared against the PoF, grate inlet 1 has showed a better performance compared to others. Grate inlet 1 produced the lowest probability of failure as compared to grate inlet 3. This is because the design of transverse grate inlet 1 has a hydraulic efficiency that could compete or

perform at the same rate as the design of the longitudinal grate inlet 3. Meanwhile, grate inlet 2 remains having the highest probability of failure among others.

It can then be concluded that when efficiency of grate inlet increased, the probability of failure decreased. Grate inlet 3 has higher probability of failure than grate inlet 1, while grate inlet 2 stay as the highest probability of failure.

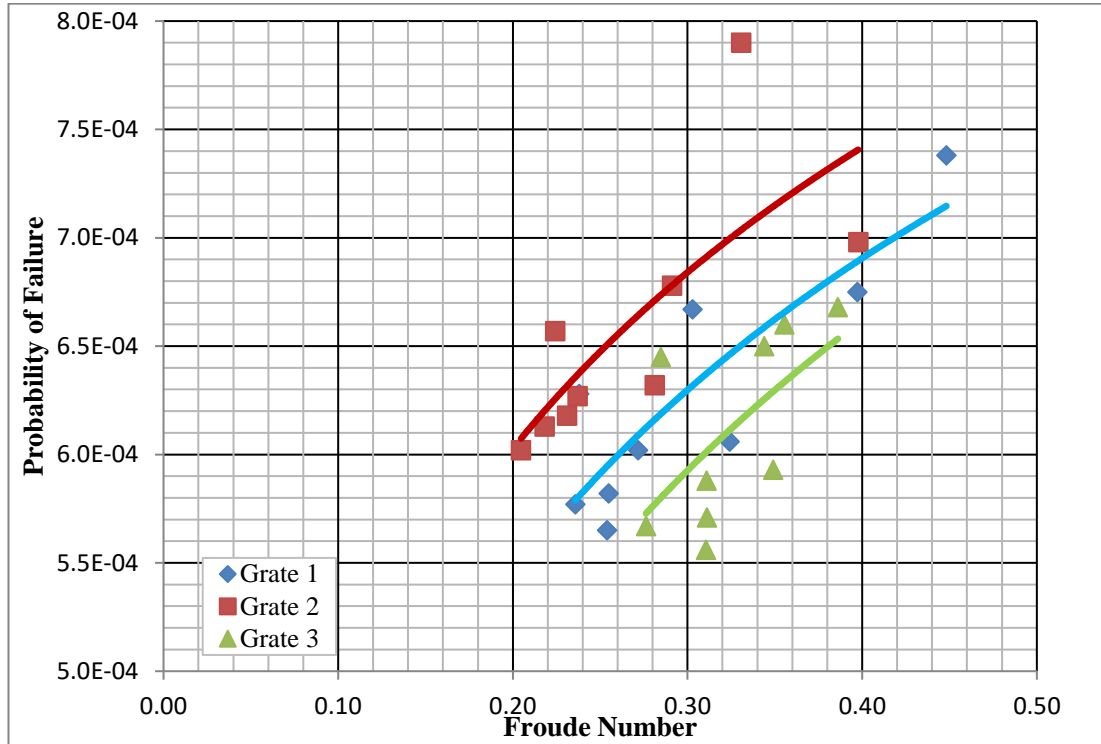


Figure 4.4: Graph of probability of failure against Froude number

Next, the effect of Froude number on probability of failure is shown in Figure 4.4. Froude number of the approaching flow was also considered because it is much related to the surface roughness, discharge and street geometry of longitudinal and transversal slope (Gomez and Russo, 2009). Froude number was calculated using Equation (2.3) and the measured Froude number from the experiment were in the range of 0.20 to 0.4. Froude number less than 1 indicated that the approaching flow was in subcritical flow condition.

Besides, from the graph showed in Figure 4.4, probability of failure increased with increased in Froude number. Grate inlet 2 having the highest probability of

failure followed by grate inlet 1 and grate inlet 3. At Froude number 0.30, PoF of grate 1, grate 2 and grate 3 was 0.00063, 0.00068 and 0.00059, respectively.

Throughout the reliability analysis conducted based on the three produced graphs of probability of failure of different grate inlets, it can be concluded that longitudinal grate inlet 1 are the most reliable, followed by transverse grate inlet 1 and transverse grate inlet 2. Therefore, by having a value of efficiency and probability of failure of the tested grate inlets, it can be used as a guide or references in design and selection of grate inlet types.

4.4 Observation

Several sets of experiments were conducted to obtain the hydraulic efficiency of three difference designs of grate inlet. In each experimental run, four things needed to be observed, namely the approaching flow, intercepted flow, bypass flow and the length of the water spread. Water flows into the supply tank, then wait around several minutes to allow uniform flow and record the heads of water from each tank and along the gutter of road flume to the grate inlet.

The approaching flows were varied from the range of $0.0003m^3/s$ to $0.022m^3/s$. It was observed that at maximum flows (Figure 4.5(a)), the nappe falls away from the weir tank as compared to minimum flow (Figure 4.5(b)).

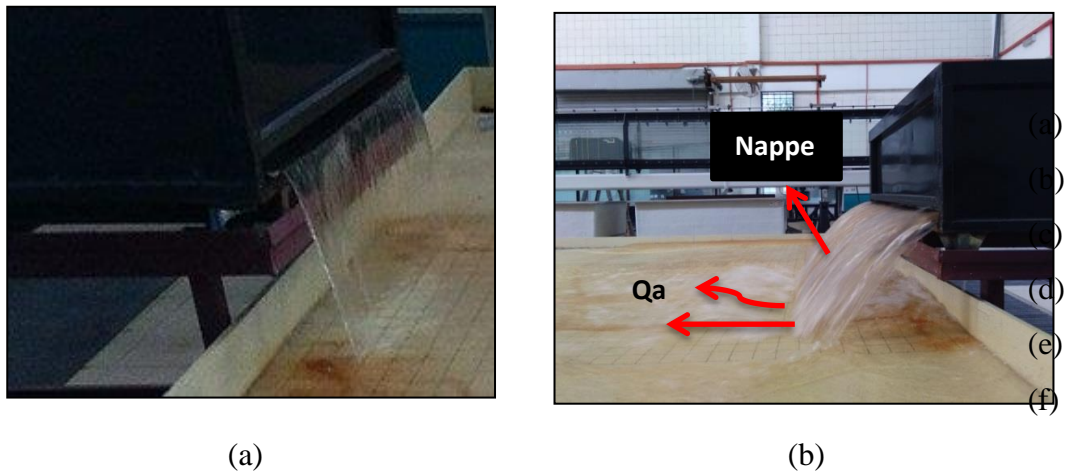


Figure 4.5: Nappe at (a) minimum flow (b) and maximum flow

Examples of approaching flows that were captured and intercepted by each of the grate inlets are shown in Figure 4.6. Throughout the experiment, it was observed that all flows intercepted by the inlet and behaved in the form of weir flow.

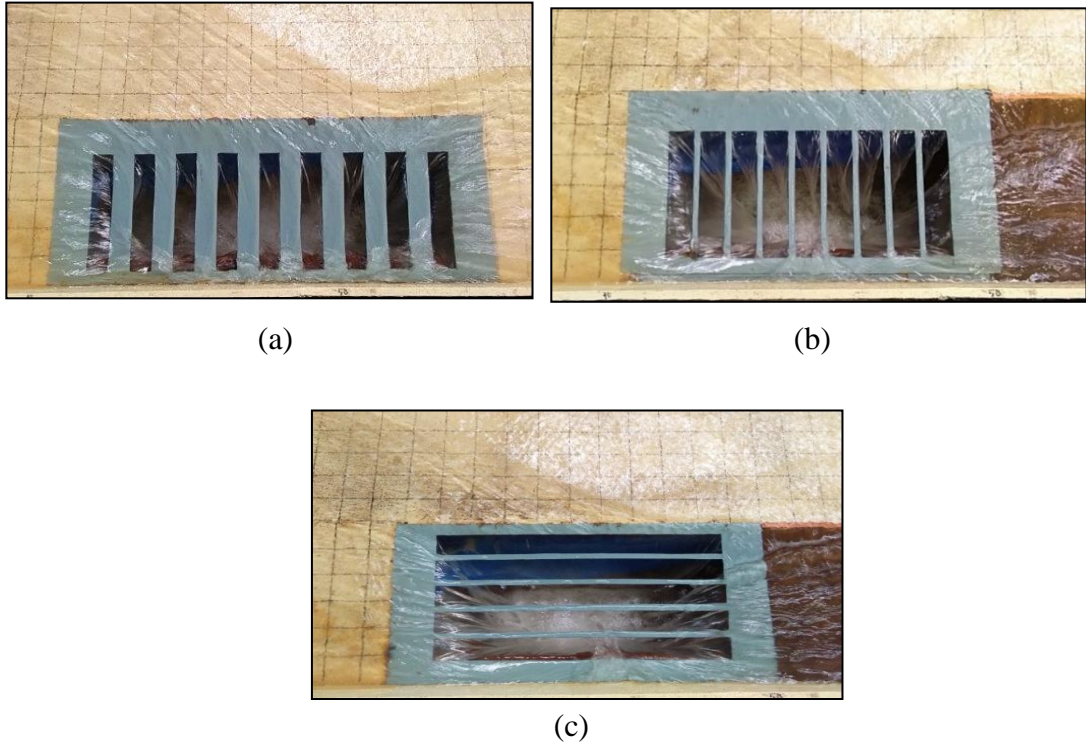


Figure 4.6: (a) grate inlet 1, (b) grate inlet 2 and (c) grate inlet 3 capturing approaching flow

Meanwhile the approaching flows that failed to be intercepted would become bypass flow and entered the bypass inlet as shown in Figure 4.7. At minimum approaching flows less than $0.0011 \text{ m}^3/\text{s}$, there was no bypass flow. When the approaching started to increase greater than $0.0011 \text{ m}^3/\text{s}$, bypass flows formed and at maximum flow it was observed that ponding occurred.

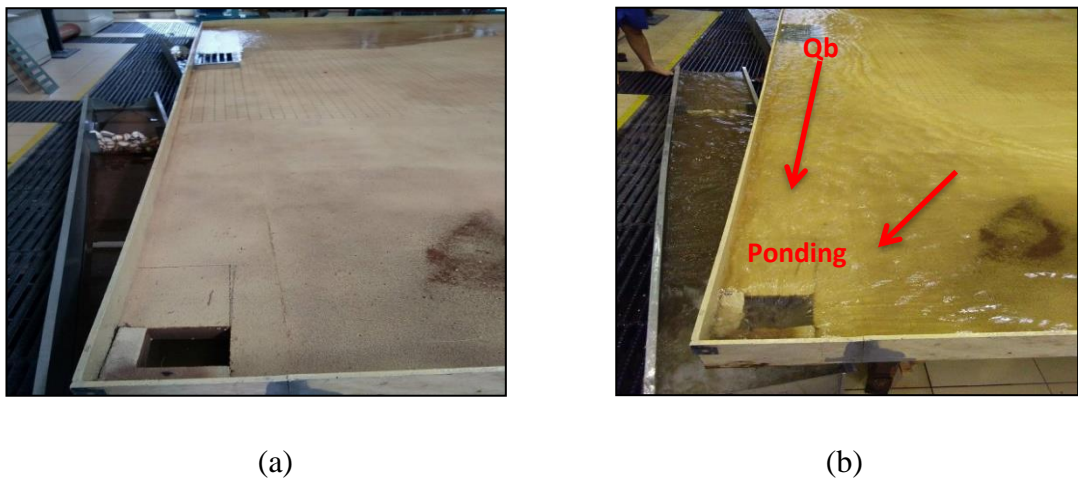


Figure 4.7: Bypass flow at (a) minimum flow and (b) maximum flow

During the experiment, three or two types of flow states could be observed as shown in Figure 4.8.

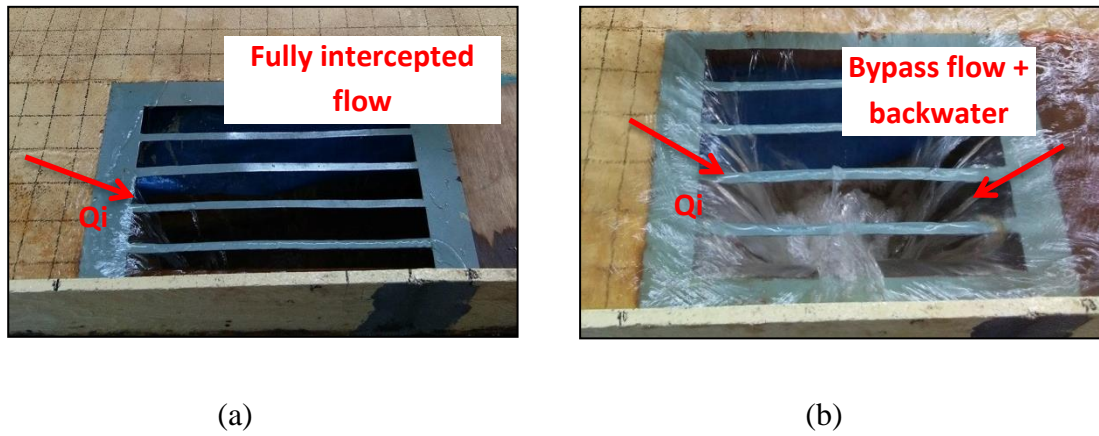


Figure 4.8: Actual flow state at (a) minimum flow and (b) maximum flow

Figure 4.9 shows an illustration of flow interception during minimum flow. It has discovered that at low flows, the approaching flow would be intercepted in the form of weir flow from one side of the grate inlets as shown in Figure 4.9(a). As such, theoretically the approaching flow was considered to be fully intercepted. As the flow discharge increased, the flow interception would come from all sides of the grate inlet as shown in Figure 4.9(b).

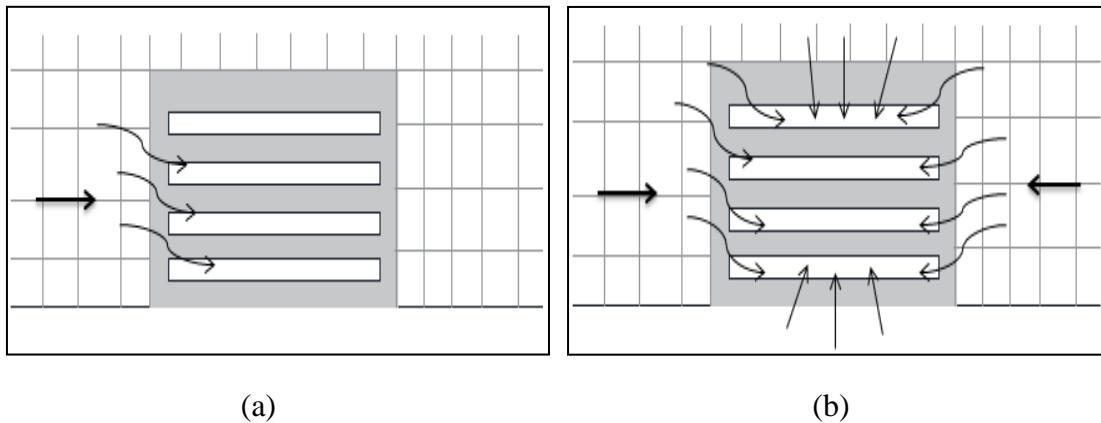


Figure 4.9: Illustration of flow interception at (a) minimum and (b) maximum flows

Figure 4.10: Actual water spreads at (a) minimum and (b) maximum flows

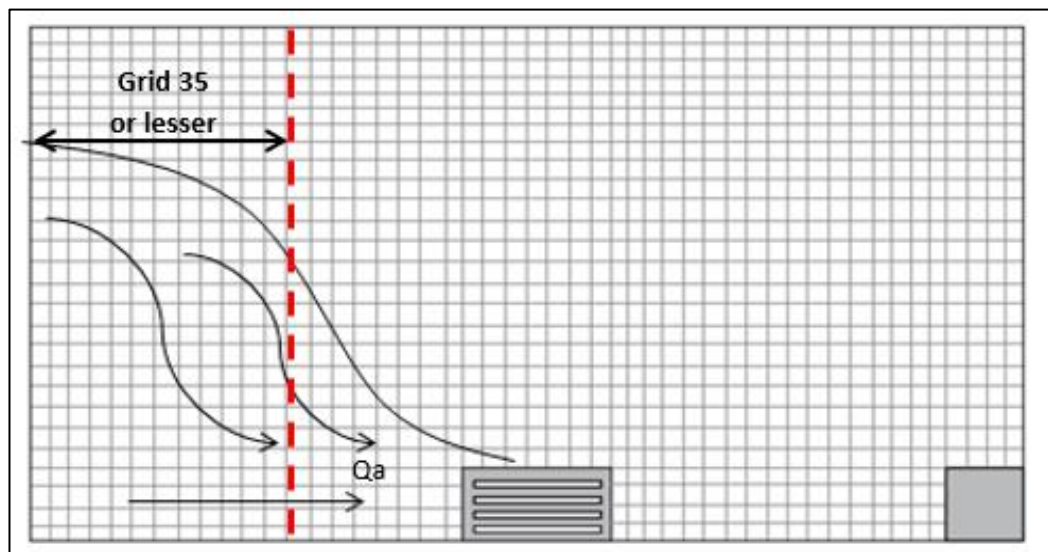


Figure 4.11: Illustration of water spreads at minimum flow

During minimum flow, it was observed that the spread of water was not too much and most of the approaching flows spread only at one side of the flume, as shown in Figure 4.11. It was found that the flows could spread around grid 35 or less and there was no bypass flow observed.

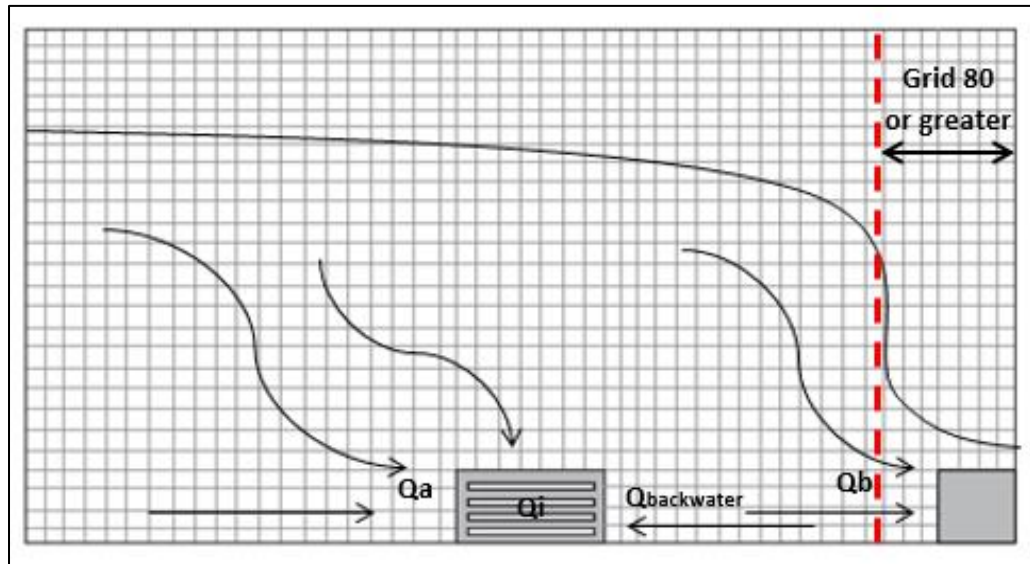


Figure 4.12: Illustration of water spread at maximum flow

In the meantime, when the approaching flows were very high closer to the maximum flow, the spread of the water was very large and covered more than half of the area of the flume as shown in Figure 4.12. The length of the spread was observed to be greater than grid 80. During high flows, most of the time backwater flows occurred. Supposedly, the water that failed to intercept would go to the bypass region but due to the spread of water was large, water accumulated at the bypass inlet and caused backwater flows. When the flows become higher, the amount of backwater also getting higher.

CHAPTER 5

CONCLUSIONS AND RECOMMENDATIONS

Inlet design is one of the factors that can affect the hydraulic efficiency of the street inlet. The study on inlet design is important in order to know the hydraulic efficiency and overcome the problem of street ponding which can cause traffic hazard to the urban street user. From the experimental studies, it shows that the length and bar configuration is a significant parameter that must be considered in the design of street inlet to capture stormwater effectively. Longer length of grate inlet can capture more flow and have performed better compare to the shorter length. Shorter grate inlet is more economical, but the design is not performing very well and satisfying during high stormwater event. Besides, this research has proven the previous research which have stated that longitudinal grate inlet has higher hydraulic efficiencies compare to transverse grate inlet.

A reliability model of probability of failure of grate inlets was successfully developed from the data obtained from experimental studies. By using limit state function (LSF), $Z = Q_{i(theory)} - Q_{i(measured)}$, a graph of probability of failure was developed from the simulation of the LSF in the MATLAB software using Monte Carlo techniques. By having the reliability model of the grate inlets, Department of Irrigation and Drainage (DID) can use it as a new guideline for inlet design and improve Manual Saliran Mesra Alam Malaysia (MSMA).

Further research on hydraulic efficiency and reliability analysis on curb opening inlet may be conducted. Then, a comparison between grate inlets and curb opening inlet can be conducted and from there the design inlet may be improved. Lastly, a research on inlet location is also recommended to see the efficiency of the inlet at certain distance.

REFERENCES

- Akan, A. O., & Houghtalen, R. J. (2007). *Urban hydrology, hydraulics, and stormwater quality: Engineering applications and computer modeling*. Hoboken: John Wiley.
- Ang, A. H.-S., & Tang, W. H. (2006). *Probability concepts in engineering planning and design: Emphasis on applications in civil & environmental engineering*. Hoboken, N.J.
- Brown, S. A., Schall, J. D., Morris, J. L., Doherty, C. L., Stein, S. M., & Warner, J. C. (2009). *Urban Drainage Design Manual Hydraulic Engineering Circular 22, Third Edition*.
- Comport, B. C., Thornton, C. I., & Cox, A. L. (2009). Hydraulic efficiency of grate and curb inlets for urban storm drainage.
- Comport, B. C., & Thornton, C. I. (2012). Hydraulic Efficiency of Grate and Curb Inlets for Urban Storm Drainage. *Journal of Hydraulic Engineering*, 138(10), 878-884. doi:10.1061/(asce)hy.1943-7900.0000552
- Despotovic, J., Plavsic, J., & Jacimovic, N. (2008). Surface runoff and safety factors for the vehicle and pedestrian street traffic.
- Guo, J. C. (1997). *Street hydraulics and inlet sizing: Using the computer model UDINLET*. Highlands Ranch: Water Resources Publications.
- Guo, J. C. (2006). Design of Street Curb Opening Inlets Using a Decay-Based Clogging Factor. *Journal of Hydraulic Engineering*, 132(11), 1237-1241. doi:10.1061/(asce)0733-9429(2006)132:11(1237)

- Guo, J. C. (2012). Hydraulic efficiency of grate and curb-opening inlets under clogging effect.
- Guo, J. C., MacKenzie, K. A., & Mommandi, A. (2009). Design of Street Sump Inlet. *Journal of Hydraulic Engineering*, 135(11), 1000-1004.
doi:10.1061/(asce)hy.1943-7900.0000094
- Gómez, M., Sánchez, H., Malgrat, P., Castillo, F., Sunyer, D., & Nanía, L. (2002). Inlet Spacing Considering the Risk Associated to Runoff. Application to Streets and Critical Points of the City of Barcelona. *Global Solutions for Urban Drainage*. doi:10.1061/40644(2002)276
- Johnson, F. L., Chang, F. F., United States, & Tye Engineering, Inc. (1984). *Drainage of highway pavements*. Springfield, VA: NTIS.
- Linsley, R. K., Franzini, J. B., & Freyberg, D. L. (1992). *Water-resources engineering*. New York: McGraw-Hill.
- Mays, L. W. (2005). *Water resources engineering*. New Jersey: John Wiley & Sons.
- Mustaffa, Z. (2011). System Reliability Assessment of Offshore Pipeline. *Ph.D, Delft. University of Technology*.
- Storm Drainage Research Committee, & Johns Hopkins University. (1956). *The design of storm-water inlets*. Baltimore.
- Urban stormwater management manual for malaysia..* (2000). Malaysia: Department of Irrigation and Drainage.
- Uyumaz, A. (1992). Discharge Capacity for Curb-Opening Inlets. *Journal of Hydraulic Engineering*, 118(7), 1048-1051. doi:10.1061/(asce)0733-9429(1992)118:7(1048)

Veerappan, R., & Le, J. (2016). Hydraulic efficiency of road drainage inlets for storm drainage system under clogging effect. *Urban Water III*.
doi:10.2495/uw160241

APPENDIX

Table A.1: Efficiency of grate inlets

Reading No.	Grate Inlet 1			Grate Inlet 2			Grate Inlet 3		
	Qi (m ³ /s)	Qa (m ³ /s)	Efficiency η (%)	Qi (m ³ /s)	Qa (m ³ /s)	Efficiency η (%)	Qi (m ³ /s)	Qa (m ³ /s)	Efficiency η (%)
1	0.0029	0.0033	0.89	0.0046	0.0062	0.74	0.0058	0.0079	0.73
2	0.0076	0.0126	0.60	0.0036	0.0046	0.78	0.0039	0.0046	0.84
3	0.0042	0.0050	0.84	0.0066	0.0106	0.62	0.0055	0.0074	0.74
4	0.0079	0.0126	0.62	0.0073	0.0121	0.60	0.0060	0.0079	0.76
5	0.0036	0.0043	0.84	0.0060	0.0087	0.69	0.0027	0.0033	0.84
6	0.0035	0.0050	0.70	0.0038	0.0054	0.71	0.0042	0.0054	0.78
7	0.0068	0.0116	0.59	0.0055	0.0092	0.60	0.0055	0.0070	0.79
8	0.0092	0.0186	0.49	0.0068	0.0142	0.48	0.0083	0.0126	0.66
9	0.0110	0.0222	0.49	0.0076	0.0216	0.35	0.0092	0.0181	0.51
10	0.0010	0.0011	0.90	0.0009	0.0011	0.88	0.0010	0.0011	0.92
11	0.0007	0.0008	0.93	0.0007	0.0008	0.91	0.0008	0.0008	0.96
12	0.0006	0.0006	0.95	0.0006	0.0006	0.93	0.0006	0.0006	0.98
13	0.0005	0.0005	0.96	0.0005	0.0005	0.93	0.0005	0.0005	0.99
14	0.0003	0.0003	1.01	0.0003	0.0003	0.97	0.0003	0.0003	1.00

Table A.2: Approaching flow and Probability of failure of grate inlets

Reading No.	Grate Inlet 1		Grate Inlet 2		Grate Inlet 3	
	Qa(m ³ /s)	PoF	Qa(m ³ /s)	PoF	Qa(m ³ /s)	PoF
1	0.0033	0.000618	0.0062	0.000664	0.0079	0.000655
2	0.0126	0.000665	0.0046	0.000636	0.0046	0.000640
3	0.0050	0.000640	0.0106	0.000685	0.0074	0.000685
4	0.0126	0.000670	0.0121	0.000692	0.0079	0.000654
5	0.0043	0.000625	0.0087	0.000673	0.0033	0.000625
6	0.0050	0.000628	0.0054	0.000657	0.0054	0.000645
7	0.0116	0.000667	0.0092	0.000678	0.0070	0.000650
8	0.0186	0.000675	0.0142	0.000698	0.0126	0.000660
9	0.0222	0.000738	0.0216	0.000790	0.0181	0.000668
10	0.0011	0.000606	0.0011	0.000632	0.0011	0.000593
11	0.0008	0.000602	0.0008	0.000627	0.0008	0.000588
12	0.0006	0.000582	0.0006	0.000613	0.0006	0.000571
13	0.0005	0.000577	0.0005	0.000602	0.0005	0.000567
14	0.0003	0.000565	0.0003	0.000618	0.0003	0.000556

Table A.3: Efficiency and Probability of failure of grate inlets

Reading No.	Grate Inlet 1		Grate Inlet 2		Grate Inlet 3	
	Efficiency η (%)	PoF	Efficiency η (%)	PoF	Efficiency η (%)	PoF
1	0.89	0.000618	0.74	0.000664	0.73	0.000655
2	0.60	0.000665	0.78	0.000636	0.84	0.000640
3	0.84	0.000640	0.62	0.000685	0.74	0.000685
4	0.62	0.000670	0.60	0.000692	0.76	0.000654
5	0.84	0.000625	0.69	0.000673	0.84	0.000625
6	0.70	0.000628	0.71	0.000657	0.78	0.000645
7	0.59	0.000667	0.60	0.000678	0.79	0.000650
8	0.49	0.000675	0.48	0.000698	0.66	0.000660
9	0.49	0.000738	0.35	0.000790	0.51	0.000668
10	0.90	0.000606	0.88	0.000632	0.92	0.000593
11	0.93	0.000602	0.91	0.000627	0.96	0.000588
12	0.95	0.000582	0.93	0.000613	0.98	0.000571
13	0.96	0.000577	0.93	0.000602	0.99	0.000567
14	1.01	0.000565	0.97	0.000618	1.00	0.000556

Table A.4: Froude number and Probability of failure of grate inlets

Reading No.	Grate Inlet 1		Grate Inlet 2		Grate Inlet 3	
	Froude No. (Fr)	PoF	No. (Fr)	PoF	No. (Fr)	PoF
1		0.000618		0.000664		0.000655
2		0.000665		0.000636		0.000640
3		0.000640		0.000685		0.000685
4		0.000670		0.000692		0.000654
5		0.000625		0.000673		0.000625
6	0.2381	0.000628	0.2242	0.000657	0.2848	0.000645
7	0.3030	0.000667	0.2912	0.000678	0.3438	0.000650
8	0.3972	0.000675	0.3977	0.000698	0.3556	0.000660
9	0.4482	0.000738	0.3307	0.000790	0.3861	0.000668
10	0.3241	0.000606	0.2812	0.000632	0.3491	0.000593
11	0.2718	0.000602	0.2371	0.000627	0.3110	0.000588
12	0.2548	0.000582	0.2182	0.000613	0.3112	0.000571
13	0.2357	0.000577	0.2047	0.000602	0.2762	0.000567
14	0.2539	0.000565	0.2310	0.000618	0.3106	0.000556